Article

Not peer-reviewed version

Analysis of the Kerr-Newman Diagram. Unravelling the Interior of a Black Hole

Hector Gerardo Flores *, Harshit Jain *, Premachand Mahapatra *, Maria Isabel Gonçalves de Souza *

Posted Date: 2 August 2024

doi: 10.20944/preprints202408.0101.v1

Keywords: RLC electrical model; RC electrical model; cosmology; astronomy; astrophysics; background radiation; Hubble's law; Boltzmann´s constant; dark energy; dark matter; black hole; Big Bang; cosmic inflation; early universe; quantum gravity; CERN; LHC; Fermilab; general relativity; particle physics; condensed matter physics; M theory; super string theory; extra dimensions; Penrose diagram, ccc conformal cyclic cosmology

 doi:10.20944/preprints202408.0101.v1

Article

Analysis of the Kerr-Newman Diagram: Unravelling the Interior of a Black Hole

Hector Gerardo Flores [1], Harshit Jain [2], Premachand Mahapatra [3] and Maria Isabel Gonçalves de Souza [4]

[1] Tucumán University, Argentina; hectorisabel2011@hotmail.com
[2] Pacif Institute of Cosmology and Selfology, India; harshit@pacif-ics.com
[3] Research Scholar: Astrophysics & Gravitational Wave Birla Institute of Technology and Science, Pilani, India Doctor of Phylosophy - PHD, Physics; p20210039@goa.bits-pilani.ac.in
[4] Universidad Federal de Campina Grande, Brazil; isa271938@hotmail.com

Abstract: Here we will explain the correlation between the Kerr-Newman diagram and the theory: RLC electrical modelling of a black hole and the early universe. We will develop a black hole model that describes and explains both theories. In the development of our analysis, we will emphasize the following conditions: $M^2 > Q^2 + a^2$, $M^2 = Q^2 + a^2$ and $M^2 < Q^2 + a^2$ and we will also analyse the condition in which the mass of a black hole reaches its critical mass $M = Mc$. We will demonstrate that the interpretation of the Kerr-Newman diagram is equivalent to the interpretation of the theory: RLC electrical modelling of a black hole and the early universe. Finally, we will generalize the proposed model for a black hole and propose a black hole model formed by negative particles, *neutroniumd*, which after reaching critical conditions of mass, pressure, volume, temperature, density, etc.; decays into a positively charged black hole, *protoniu*. Let us remember that both models are formed by charged particles of matter (they do not contain antimatter), but their vector configuration means that the net charges of both proposed black holes are zero.

Keywords: RLC electrical model; RC electrical model; cosmology; astronomy; astrophysics; background radiation; Hubble's law; Boltzmann´s constant; dark energy; dark matter; black hole; Big Bang; cosmic inflation; early universe; quantum gravity; CERN; LHC; Fermilab; general relativity; particle physics; condensed matter physics; M theory; super string theory; extra dimensions; Penrose diagram; ccc conformal cyclic cosmology

1. Introduction

Here, we are going to use the theory developed in the article: RLC Electrical Modelling of Black Hole and Early Universe. Generalization of the Boltzmann constant in curved spacetime.

Understanding the fundamental concepts of this theory is very important, it will allow us to make a correlation with the theory that describes the Newman-Kerr diagram for a rotating and charged black hole.

It is important to highlight that the mathematics involved in the Schwarzschild metric, the Kerr metric, the Reissner-Nordström metric or eventually the Newman-Kerr metric, are not objective and are subject to interpretations with a wide margin of uncertainty due to our lack of exact knowledge. Expressions such as our universe, parallel universe, wormhole, parallel wormhole, antiverse, etc. appear; with which we identify the different areas of the Penrose diagram.

In this paper, we will use the theory: electrical modelling of a black hole and the early universe, to objectively define the different regions represented in the Penrose diagram. We will demonstrate that a white hole originates when a black hole decays; This event begins cosmic inflation.

We will also give an adequate physical interpretation when we talk about negative mass, we will discover its true meaning and how it is related to cosmic inflation.

The Penrose Property with a Cosmological Constant

Before beginning our analysis, we are going to make a reference to the paper entitled: *The Penrose Property with a Cosmological Constant*; which provides us with a description of the characteristics of

 doi:10.20944/preprints202408.0101.v1

space-time, according to the cosmological constant being $\Lambda > 0$, $\Lambda = 0$, $\Lambda < 0$, with respect to its mass, $m > 0$, $m = 0$ and $m < 0$.

We can represent this in the following table:

Table 1. Space-time dimension vs cosmological constant for: $m > 0$, $m = 0$ and $m < 0$.

	$\Lambda = 0$			$\Lambda > 0$			$\Lambda < 0$		
Spacetime dimension	$m > 0$	$m = 0$	$m < 0$	$m > 0$	$m = 0$	$m < 0$	$m > 0$	$m = 0$	$m < 0$
3	✓	✗	✗	-	✗	-	-	✗	-
4	✓	✗	✗	✓	✗	✗	✗	✗	✓
≥ 5	✗	✗	✗	✓	✗	✗	✗	✗	✓

where a dash indicates that this spacetime has not been considered here.

A detailed analysis of the equations that demonstrate the results of Table 1 can be seen in the paper: *The Penrose Property with a Cosmological Constant*

In Table 1, it is observed, for a space-time anti de Sitter ADS ($\Lambda < 0$), of dimension $n > 3$, the Penrose property is satisfied for: $m < 0$.

Next, we are going to analyse a very important segment of the conclusion of the paper: *The Penrose Property with a Cosmological Constant,* which is related to what is shown in Table 1:

In order to rule out a formulation of quantum gravity based on a fixed background Minkowski spacetime, Penrose showed in [16] that it was sufficient to find one physically relevant spacetime which satisfies the non-timelike boundary version of the Penrose property. For asymptotically de Sitter spacetimes, the Schwarzschild-de Sitter black hole satisfies this property and hence rules out a SO(d+11) covariant construction of quantum gravity based on a background de Sitter spacetime. Note that unlike in the asymptotically at case, such a construction is ruled out in d+1 dimensions for any d > 3. For asymptotically anti-de Sitter spacetimes we can rule out a quantum gravity construction if we are able to find a physically relevant spacetime satisfying the timelike boundary version of the Penrose property (Definition 2.9). However, the spacetime we have found which satisfies this is the negative mass Schwarzschild-AdS spacetime which we may regard as not being physically relevant. Furthermore, the Theorem of Gao and Wald (Theorem 2.10) shows that this property fails for spacetimes which focus null geodesics. These are spacetimes we would like to regard as physical since they are associated with spacetimes containing positive energy densities. As a result, we are unable to rule out a quantum gravity construction based on a fixed background anti-de Sitter spacetime.

In this segment of the conclusion, we are going to highlight the following:

However, the spacetime we have found which satisfies this is the negative mass Schwarzschild-AdS spacetime which we may regard as not being physically relevant.

I want to get to this point precisely; If we look at Table 1 and consider the negative mass as not relevant, I think it is a very serious error.

It is here, where the theory: *RLC electrical modelling of a black hole and the universe*, appears and becomes relevant.

Which proposes the following:

We will consider the total mass of a black hole to consist of the sum of baryonic mass and dark matter mass, considering dark matter as an imaginary number.

$$M = m - i\delta$$

which we can write in the following way:

$$M = m + i(-\delta)$$

Where M is the total mass of a black hole, m is the baryonic mass; δ corresponds to dark matter and i is the irrational number $\sqrt{-1}$. This equation is in analogy to impedance of an RC circuit.

$$Z = R - iX_c$$

Where Z represents impedance; R represents resistance and Xc represents reactance.

Here we put forward the hypothesis that the big bang is the convolution of the energy released by disintegration of the black hole with the space-time surrounding the black hole, being defined as:

$$(m - i\delta) * \mathcal{E}$$

Where $m - i\delta$, is the total mass of a black hole, $\mathcal{E}$ is the space-time surrounding the black hole and * is the convolution symbol.

 doi:10.20944/preprints202408.0101.v1

We can simplify it and consider it analogous to an RLC circuit.

Where RC represents a black hole and L represents the space-time around a black hole.

$$RC = m - i\delta$$
$$L = \mathcal{E}$$

the resolution of the quadratic equation of the RLC circuit will determine how space-time will expand after the Big Bang and the bandwidth of the equation will give us the spectrum of gravitational waves that originated during the Big Bang.

Briefly, we have described the theory: RLC electrical modelling of a black hole and the early universe.

We can see that the definition of a black hole contains negative mass, which is very relevant; It determines the relativistic mass of the dark matter contained inside a black hole.

Just as a capacitor stores electrical energy, in analogy, we can consider a black hole as a capacitor that stores gravitational potential energy.

Just as a capacitor is made up of a real part and a negative imaginary part, analogously, the physical idea of considering a black hole formed by a baryon mass and a negative mass or negative imaginary mass, depending on how we consider it, is physically possible.

The analysis carried out by Dr Peter Cameron, which is represented in Table 1, is of utmost importance, will allow us to carry out a new interpretation of the extended Kerr-Newman diagram using the theory of the paper: *Rlc Electrical Modelling of Black Hole and Early Universe. Generalization of Boltzmann's Constant in Curved Space-Time; for a space-time anti de Sitter ADS ($\Lambda < 0$) of dimension $n > 3$, for $m < 0$.*

It is also important to highlight the conditions:

- $\Lambda = 0$; n = 3, 4 and m > 0
- $\Lambda > 0$; n > 3 and m > 0

These conditions are very relevant in flat space-time ($\Lambda = 0$) and de Sitter space-time ($\Lambda > 0$).

In analogy to what happens in a curved space-time ($\Lambda < 0$); in a flat space-time ($\Lambda = 0$) and in a de Sitter space-time ($\Lambda > 0$), there is a force tangential to the force of gravitational attraction, which makes a body rotate clockwise.

In the case of a black hole, the tangential force generated by dark matter causes the black hole to rotate counter-clockwise. In the case of particle disintegrations, the particles experience a repulsion force and a tangential force that causes them to rotate clockwise.

This is demonstrated in the paper: Rlc Electrical Modelling of Black Hole and Early Universe. Generalization of Boltzmann's Constant in Curved Space-Time.

2. Kerr-Newman Black Hole

The importance of the Kerr-Newman geometry stems in part from the no-hair theorem, which states that this geometry is the unique end state of spacetime outside the horizon of an undisturbed black hole in asymptotically at space.

2.1. Boyer-Lindquist metric

The Boyer-Lindquist metric of the Kerr-Newman geometry is:

$$ds^2 = -\frac{R^2\Delta}{\rho^2}\left(dt - a\sin^2\theta\, d\phi\right)^2 + \frac{\rho^2}{R^2\Delta}dr^2 + \rho^2 d\theta^2 + \frac{R^4\sin^2\theta}{\rho^2}\left(d\phi - \frac{a}{R^2}dt\right)^2 \quad (1)$$

where R and are defined by:

$$R \equiv \sqrt{r^2 + a^2}\,, \quad \rho \equiv \sqrt{r^2 + a^2\cos^2\theta}\,, \quad (2)$$

And Δ is the horizon function defined by:

$$\Delta \equiv 1 - \frac{2Mr}{R^2} + \frac{Q^2}{R^2}\,. \quad (3)$$

 doi:10.20944/preprints202408.0101.v1

If M = Q = 0, so that Δ = 1, the Boyer-Lindquist metric (1) goes over to the metric of Minkowski space expressed in ellipsoidal coordinates

At large radius r, the Boyer-Lindquist metric is

$$ds^2 \to -\left(1-\frac{2M}{r}\right)dt^2 - \frac{4aM\sin^2\theta}{r}dtd\phi + \left(1+\frac{2M}{r}\right)dr^2 + r^2\left(d\theta^2+\sin^2\theta\, d\phi^2\right) \quad (4)$$

The weak- field metric in Newtonian gauge, around an object of mass M and angular momentum L takes the form:

$$ds^2 = -(1+2\Psi)dt^2 - 2Wr\sin\theta\, dtd\phi + (1-2\Phi)(dr^2+r^2do^2)\ , \quad (5)$$

Where, the scalar ϕ, ψ and vector W potentials are:

$$\Psi = \Phi = -\frac{M}{r}\ , \quad W = -\frac{2L\sin\theta}{r^2}\ . \quad (6)$$

The asymptotic Boyer-Lindquist metric (4) is not quite in the Newtonian form (5), but a transformation of the radial coordinate brings it to Newtonian form. Comparison of the two metrics establishes that M is the mass of the black hole and a = L/M is its angular momentum per unit mass. For positive a, the black hole rotates right-handedly about its polar axis $\phi = 0$.

The Boyer-Lindquist line-element (1) defines not only a metric but also a tetrad. The Boyer-Lindquist coordinates and tetrad are carefully chosen to exhibit the symmetries of the geometry. In the locally inertial frame defined by the Boyer-Lindquist tetrad, the energy-momentum tensor (which is non-vanishing for charged Kerr-Newman) and the Weyl tensor are both diagonal. These assertions become apparent only in the tetrad frame and are obscure in the coordinate frame.

2.2. Oblate Spheroidal Coordinates

Boyer-Lindquist coordinates *r*, ϕ, θ are oblate spheroidal coordinates (not polar coordinates). Corresponding Cartesian coordinates are:

$$\begin{aligned} x &= R\sin\theta\cos\phi\ , \\ y &= R\sin\theta\sin\phi\ , \\ z &= r\cos\theta\ . \end{aligned} \quad (7)$$

Surfaces of constant r, are confocal oblate spheroids, satisfying

$$\frac{x^2+y^2}{R^2}+\frac{z^2}{r^2}=1\ . \quad (8)$$

Equation (39) implies that the spheroidal coordinate r is given in terms of x, y, z by the quadratic equation:

$$r^4 - r^2(x^2+y^2+z^2-a^2) - a^2z^2 = 0\ . \quad (9)$$

Figure 1, illustrates the spatial geometry of a Kerr black hole, and of a Kerr-Newman black hole, in Boyer-Lindquist coordinates.

 doi:10.20944/preprints202408.0101.v1

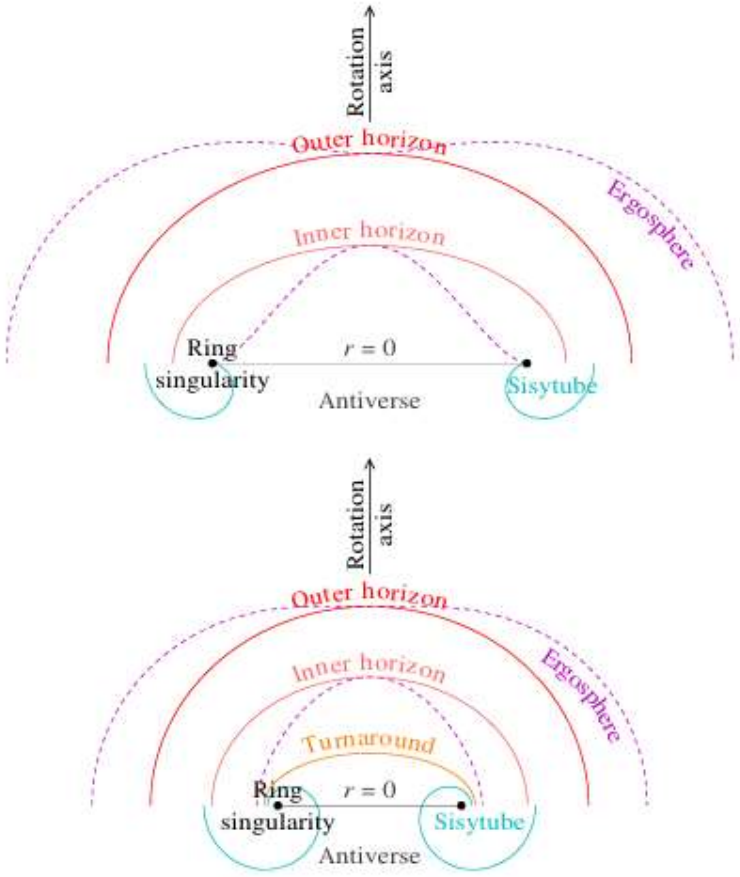

Figure 1. Spatial geometry of (upper) a Kerr black hole with spin parameter a = 096M, and (lower) a Kerr-Newman black hole with charge Q = 08M and spin parameter a = 056M. The upper half of each diagram shows r ≥ 0, while the lower half shows r ≤ 0, the Antiverse. The outer and inner horizons are confocal oblate spheroids whose focus is the ring singularity. For the Kerr geometry, the turnaround radius is at r = 0. The Sisytube is a torus enclosing the ring singularity, that contains closed time like curves.

2.3. Time and Rotation Symmetries

The Boyer-Lindquist metric coefficients are independent of the time coordinate t and of the azimuthal angle ϕ. This shows that the Kerr-Newman geometry has time translation symmetry, and rotational symmetry about its azimuthal axis. The time and rotation symmetries mean that the tangent vectors e(t) and e(ϕ) in Boyer-Lindquist coordinates are Killing vectors. It follows that their scalar products:

$$\begin{aligned} \boldsymbol{e}_t \cdot \boldsymbol{e}_t = g_{tt} &= -\frac{1}{\rho^2}\left(R^2\Delta - a^2\sin^2\theta\right) , \\ \boldsymbol{e}_t \cdot \boldsymbol{e}_\phi = g_{t\phi} &= -\frac{aR^2\sin^2\theta}{\rho^2}\left(1-\Delta\right) , \\ \boldsymbol{e}_\phi \cdot \boldsymbol{e}_\phi = g_{\phi\phi} &= \frac{R^2\sin^2\theta}{\rho^2}\left(R^2 - a^2\sin^2\theta\,\Delta\right) , \end{aligned} \tag{10}$$

are all gauge-invariant scalar quantities. As will be seen below, gtt = 0 defines the boundary of ergospheres, $gt\phi = 0$ defines the turnaround radius, and $g\phi\phi = 0$ defines the boundary of the sisytube, the toroidal region containing closed time like curves.

The Boyer-Lindquist time t and azimuthal angle ϕ are arranged further to satisfy the condition that e(t) and e(ϕ) are each orthogonal to both e(r) and e(θ).

 doi:10.20944/preprints202408.0101.v1

2.4. Ring Singularity

The Kerr-Newman geometry contains a ring singularity where the Weyl tensor (9.26) diverges, ϱ = 0, or equivalently at

$$\boxed{r = 0 \text{ and } \theta = \pi/2} \ . \tag{11}$$

The ring singularity is at the focus of the confocal ellipsoids of the Boyer-Lindquist metric. Physically, the singularity is kept open by the centrifugal force.

Figure 2, illustrates contours of constant in a Kerr black hole.

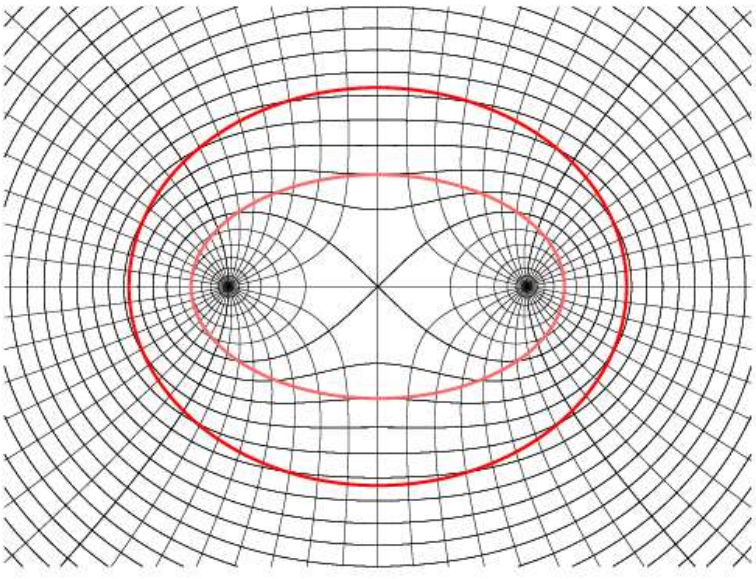

Figure 2. Not a mouse's eye view of a snake coming down its mousehole, uhoh. Contours of constant ρ and their covariant normal ($d\rho$ / dx^{μ}) in a spatial cross-section of a Kerr black hole of spin parameter a = 096M, in Boyer Lindquist coordinates. The thicker contours are the outer and inner horizons, which are confocal spheroids with the ring singularity at their focus. The ring singularity is at $\rho = 0$, the snake's eyes.

2.5. Horizons

The horizon of a Kerr-Newman black hole rotates, as observed by a distant observer, so it is incorrect to try to solve for the location of the horizon by assuming that the horizon is at rest. The worldline of a photon that sits on the horizon, battling against the in ow of space, remains at fixed radius r and polar angle θ, but it moves in time t and azimuthal angle ϕ. The photon's 4-velocity is $v^{\mu} = \{v^t, 0, 0, v^{\phi}\}$, and the condition that it is on a null geodesic is:

$$0 = v_{\mu} v^{\mu} = g_{\mu\nu} v^{\mu} v^{\nu} = g_{tt} (v^t)^2 + 2\, g_{t\phi}\, v^t v^{\phi} + g_{\phi\phi} (v^{\phi})^2 \ . \tag{12}$$

This equation has solutions provided that the determinant of the 2 x 2 matrix of metric coefficients in t and ϕ is less than or equal to zero (why?). The determinant is:

$$g_{tt} g_{\phi\phi} - g_{t\phi}^2 = -R^2 \sin^2\theta\, \Delta \ , \tag{13}$$

where is the horizon function defined above, equation (34). Thus, if Δ ≥ 0, then there exist null geodesics such that a photon can be instantaneously at rest in r and θ, whereas if Δ < 0, then no such geodesics exist. The boundary

$$\Delta = 0 \tag{14}$$

defines the location of horizons. With Δ given by equation (3), equation (14) gives outer and inner horizons at:

 doi:10.20944/preprints202408.0101.v1

$$\boxed{r_{\pm} = M \pm \sqrt{M^2 - Q^2 - a^2}} \ . \tag{15}$$

Between the horizons Δ is negative, and photons cannot be at rest. This is consistent with the picture that space is falling faster than light between the horizons.

2.6. Angular Velocity of the Horizon

The angular velocity of the horizon as observed by observers at rest at infinity can be read o directly from the Boyer-Lindquist metric (1). The horizon is at $dr = d\theta = 0$ and $\Delta = 0$, and then the null condition $ds^2 = 0$ implies that the angular velocity is

$$\frac{d\phi}{dt} = \frac{a}{R^2} \ . \tag{16}$$

The derivative is with respect to the proper time t of observers at rest at infinity, so this is the angular velocity observed by such observers

2.7. Ergospheres

There are finite regions, just outside the outer horizon and just inside the inner horizon, within which the worldline of an object at rest, $dr = d\theta = d\phi = 0$, is spacelike. These regions, called ergospheres, are places where nothing can remain at rest (the place where little children come from). Objects can escape from within the outer ergosphere (whereas they cannot escape from within the outer horizon), but they cannot remain at rest there. A distant observer will see any object within the outer ergosphere being dragged around by the rotation of the black hole. The direction of dragging is the same as the rotation direction of the black hole in both outer and inner ergospheres.

The boundary of the ergosphere is at

$$g_{tt} = 0 \ , \tag{17}$$

which occurs where:

$$R^2\Delta = a^2 \sin^2\theta \ . \tag{18}$$

Equation (18) has two solutions, the outer and inner ergospheres. The outer and inner ergospheres touch respectively the outer and inner horizons at the poles, $\theta = 0$ and π.

2.8. Turnaround Radius

The turnaround radius is the radius inside the inner horizon at which infallers who fall from zero velocity and zero angular momentum at infinity turn around. The radius is at:

$$g_{t\phi} = 0 \ , \tag{19}$$

which occurs where $\Delta = 1$, or equivalently at:

$$r = \frac{Q^2}{2M} \ . \tag{20}$$

In the uncharged Kerr geometry, the turnaround radius is at zero radius, $r = 0$, but in the Kerr-Newman geometry the turnaround radius is at positive radius.

2.9. Antiverse

The surface at zero radius, $r = 0$, forms a disk bounded by the ring singularity. Objects can pass through this disk into the region at negative radius, $r < 0$, the Antiverse.

The Boyer-Lindquist metric (1) is unchanged by a symmetry transformation that simultaneously flips the sign both of the radius and mass, $r \rightarrow -r$ and $M \rightarrow -M$. Thus, the Boyer-Lindquist geometry at negative r with positive mass is equivalent to the geometry at positive r with negative mass. In effect, the Boyer-Lindquist metric with negative r describes a rotating black hole of negative mass

 doi:10.20944/preprints202408.0101.v1

$$M < 0 \qquad (21)$$

2.10. Sisytube

Inside the inner horizon there is a toroidal region around the ring singularity, which I call the sisytube, within which the light cone in t-ϕ coordinates opens up to the point that ϕ as well as t is a time like coordinate. In the Wormhole, the direction of increasing proper time along t is t increasing, and along ϕ is ϕ decreasing, which is retrograde. In the Parallel Wormhole, the direction of increasing proper time along t is t decreasing, and along ϕ is ϕ increasing, which is again retrograde. Within the toroidal region, there exist time like trajectories that go either forwards or backwards in coordinate time t as they wind retrograde around the toroidal tunnel. Because the ϕ coordinate is periodic, these time-like curves connect not only the past to the future (the usual case), but also the future to the past, which violates causality. In particular, as rst pointed out by Carter (1968), there exist closed time like curves (CTCs), trajectories that connect to themselves, connecting their own future to their own past, and repeating interminably, like Sisyphus pushing his rock up the mountain.

The boundary of the sisytube torus is at:

$$g_{\phi\phi} = 0 \ , \qquad (22)$$

which occurs where:

$$R^2 = a^2 \sin^2\theta \, \Delta \ . \qquad (23)$$

In the uncharged Kerr geometry, the sisytube is entirely at negative radius, r < 0, but in the Kerr-Newman geometry the sisytube extends to positive radius, Figure 1.

2.11. Extremal Kerr-Newman Geometry

The Kerr-Newman geometry is called extremal when the outer and inner horizons coincide, r+ = r-, which occurs where:

$$M^2 = Q^2 + a^2 \ . \qquad (24)$$

Figure 3, illustrates the structure of an extremal Kerr (uncharged) black hole and an extremal Kerr-Newman (charged) black hole.

Preprints.org (www.preprints.org) | NOT PEER-REVIEWED | Posted: 2 August 2024 doi:10.20944/preprints202408.0101.v1

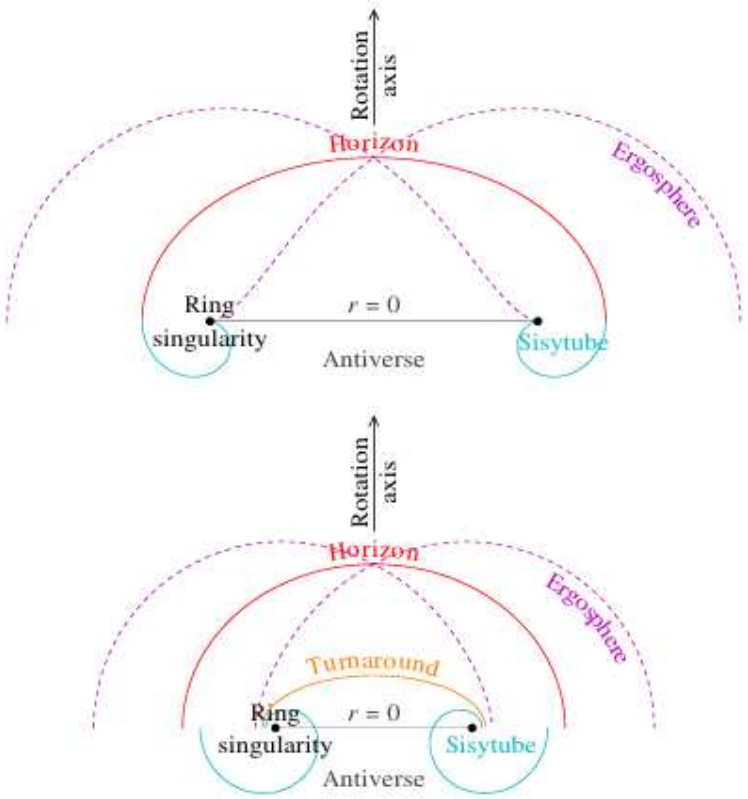

Figure 3. Spatial geometry of (upper) an extremal (a=M) Kerr black hole, and (lower) an extremal Kerr-Newman black hole with charge Q = 08M and spin parameter a = 06M.

2.12. Super-extremal Kerr-Newman Geometry

If $M^2 < Q^2 + a^2$, then there are no horizons. The geometry is called super-extremal. Figure 4, illustrates the structure of a super-extremal Kerr black hole. A super-extremal black hole has a naked ring singularity, and CTCs in a sisytube unhidden by a horizon.

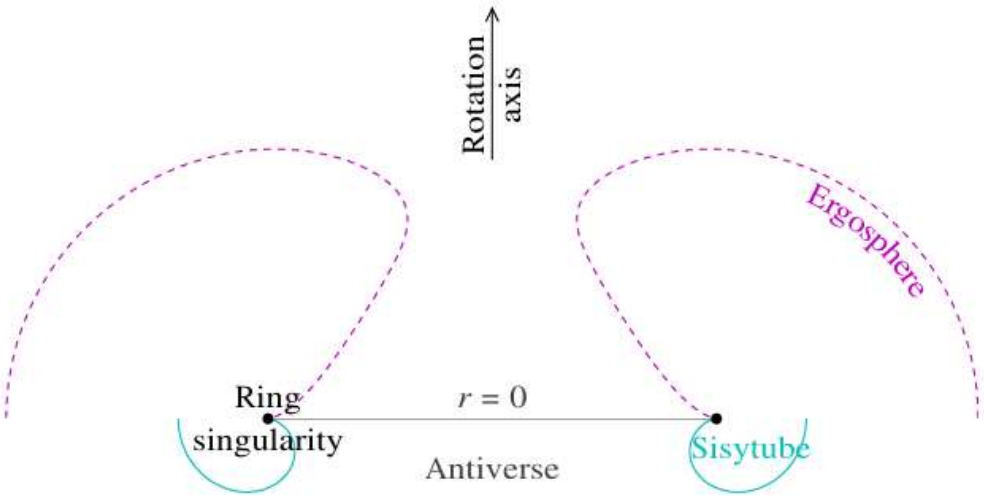

Figure 4. Spatial geometry of a super-extremal Kerr black hole with spin parameter a = 104M. A super-extremal black hole has no horizons.

 doi:10.20944/preprints202408.0101.v1

2.13. Energy-Momentum Tensor

The coordinate-frame Einstein tensor of the Kerr-Newman geometry in Boyer-Lindquist coordinates is a bit of a mess. The trick of raising one index, which for the Reissner-Nordström metric brought the Einstein tensor to diagonal form, equation (5), fails for Boyer-Lindquist (because the Boyer-Lindquist metric is not diagonal). The problem is endemic to the coordinate approach to general relativity. After tetrads it will emerge that, in the Boyer-Lindquist tetrad, the Einstein tensor is diagonal, and that the proper density ρ, the proper radial pressure p(r), and the proper transverse pressure p(⊥) in that frame are (do not confuse the notation ρ for proper density with the radial parameter ρ, equation (2), of the Boyer-Lindquist metric).

$$\rho = -p_r = p_\perp = \frac{Q^2}{8\pi\rho^4} \ . \tag{25}$$

This looks like the energy-momentum tensor of the Reissner-Nordström geometry with the replacement r → ϱ. The energy-momentum is that of an electric field produced by a charge Q seemingly located at the ring singularity.

2.14. Weyl Tensor

The Weyl tensor of the Kerr-Newman geometry in Boyer-Lindquist coordinates is likewise a mess. After tetrads, it will emerge that the 10 components of the Weyl tensor can be decomposed into 5 complex components of spin 0, ±1, and ±2. In the Boyer-Lindquist tetrad, the only non-vanishing component is the spin-0 component, the Weyl scalar C, but in contrast to the Schwarzschild and Reissner-Nordström geometries the spin-0 component is complex, not real:

$$C = -\frac{1}{(r - ia\cos\theta)^3}\left(M - \frac{Q^2}{r + ia\cos\theta}\right) \ . \tag{26}$$

2.15. Electromagnetic Field

The expression for the electromagnetic eld in Boyer-Lindquist coordinates is again a mess. After tetrads, it will emerge that, in the Boyer-Lindquist tetrad, the electromagnetic field is purely radial, and the electromagnetic potential has only a time component. For reference, the covariant electromagnetic potential Au in the Boyer-Lindquist coordinate (not tetrad) frame is:

$$A_\mu = \frac{Qr}{\rho^2}\left\{-1,\ 0,\ 0,\ \frac{a\sin\theta}{R\sqrt{\Delta}}\right\} \ . \tag{27}$$

2.16. Principal Null Congruences

The Kerr-Newman geometry admits a special set of space-filling, non-overlapping null geodesics called the principal outgoing and ingoing null congruences. These are the directions with respect to which the Weyl tensor and the electric field vector align. Photons that hold steady on the outer horizon are on the principal outgoing null congruence. The construction and special character of the principal null congruences will be demonstrated after tetrads.

Geodesics along the principal null congruences satisfy:

$$d\theta = d\phi - \omega\, dt = 0 \ , \tag{28}$$

where w = a / R² is the azimuthal angular velocity of the geodesics through the coordinates. The Boyer Lindquist line-element (1) is specifically constructed so that it aligns with the principal null congruences.

2.17. Finkelstein Coordinates

Along the principal outgoing and ingoing null congruences, where equations (28) hold, the Boyer-Lindquist metric (32) reduces to:

 doi:10.20944/preprints202408.0101.v1

$$ds^2 = \frac{\rho^2 \Delta}{R^2}\left(-dt^2 + \frac{dr^2}{\Delta^2}\right) . \tag{29}$$

A tortoise coordinate r* in the Kerr-Newman geometry may be defined analogously to that (16) in the Reissner-Nordström geometry,

$$r^* \equiv \int \frac{dr}{\Delta} , \tag{30}$$

which integrates to the same expressions in terms of horizon radii $r\pm$ and surface gravities $k\pm$ as in the Reissner-Nordström geometry. Principal outgoing and ingoing null geodesics follow

$$\begin{aligned} r^* - t &= \text{constant} \quad \text{outgoing} , \\ r^* + t &= \text{constant} \quad \text{ingoing} . \end{aligned} \tag{31}$$

A Finkelstein time coordinate tF can be defined as in the Reissner-Nordström geometry. Likewise, Kruskal-Szekeres coordinates can be defined as in the Reissner-Nordström geometry. The Finkelstein and Kruskal spacetime diagrams for the Kerr-Newman geometry look identical to those of the Reissner-Nordström geometry (if the horizon radii r± are the same).

The behaviour of geodesics in the angular direction is more complicated in the Kerr-Newman than Reissner Nordström geometry, but this complexity is hidden in the Finkelstein and Kruskal diagrams

2.18. Doran Coordinates

For the Kerr-Newman geometry, the analogue of the Gullstrand-Painlevé metric is the Doran (2000) metric:

$$\boxed{ds^2 = -dt_{\rm ff}^2 + \left[\frac{\rho}{R}dr - \beta\frac{R}{\rho}\left(dt_{\rm ff} - a\sin^2\theta\, d\phi_{\rm ff}\right)\right]^2 + \rho^2 d\theta^2 + R^2\sin^2\theta\, d\phi_{\rm ff}^2} \tag{32}$$

where the free-fall time t(H) and azimuthal angle $\phi(H)$ are related to the Boyer-Lindquist time t and azimuthal angle ϕ by:

$$dt_{\rm ff} = dt - \frac{\beta}{1-\beta^2}dr , \quad d\phi_{\rm ff} = d\phi - \frac{a\beta}{R^2(1-\beta^2)}dr . \tag{33}$$

The free-fall time t(H) is the proper time experienced by persons who free-fall from rest at infinity, with zero angular momentum. They follow trajectories of fixed θ and ϕ(H), with radial velocity dr / dt = $\beta R^2/\varrho^2$. The 4-velocity $u^\nu \equiv dx^\nu/d\tau$ of such free-falling observers is:

$$u^{t_{\rm ff}} = 1 , \quad u^r = \frac{R^2\beta}{\rho^2} , \quad u^\theta = 0 , \quad u^{\phi_{\rm ff}} = 0 . \tag{34}$$

 doi:10.20944/preprints202408.0101.v1

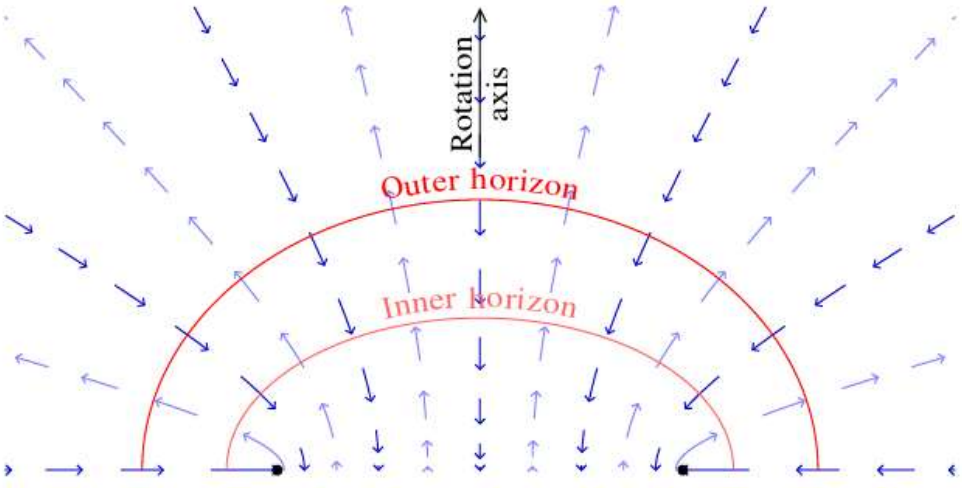

Figure 5. Spatial geometry of a Kerr black hole with spin parameter a=096M. The arrows show the velocity β in the Doran metric. The flow follows lines of constant, which form nested hyperboloids orthogonal to and confocal with the nested spheroids of constant r.

For the Kerr-Newman geometry, the velocity β is:

$$\beta = \mp \frac{\sqrt{2Mr - Q^2}}{R} \tag{35}$$

Where the ± sign is - (infalling) for black hole solutions, and+ (outfalling) for white hole solutions. Horizons occur where the magnitude of the velocity β equals the speed of light.

$$\beta = \mp 1 \ . \tag{36}$$

The boundaries of ergospheres occur where the velocity is:

$$\beta = \mp \frac{\rho}{R} \ . \tag{37}$$

The turnaround radius is where the velocity is zero

$$\beta = 0 \tag{38}$$

The sisytube is bounded by the imaginary velocity:

$$\beta = i \frac{\rho}{a \sin \theta} \ . \tag{39}$$

2.19. Penrose Diagram

The Penrose diagram of the Kerr-Newman geometry, Figure 6, resembles that of the Reissner-Nordström geometry, except that in the Kerr-Newman geometry an infaller can reach the Antiverse by passing through the disk at r = 0 bounded by the ring singularity. In the Reissner-Nordström geometry, the ring singularity shrinks to a point, and passing into the Antiverse would require passing through the singularity itself.

Preprints.org (www.preprints.org) | NOT PEER-REVIEWED | Posted: 2 August 2024 doi:10.20944/preprints202408.0101.v1

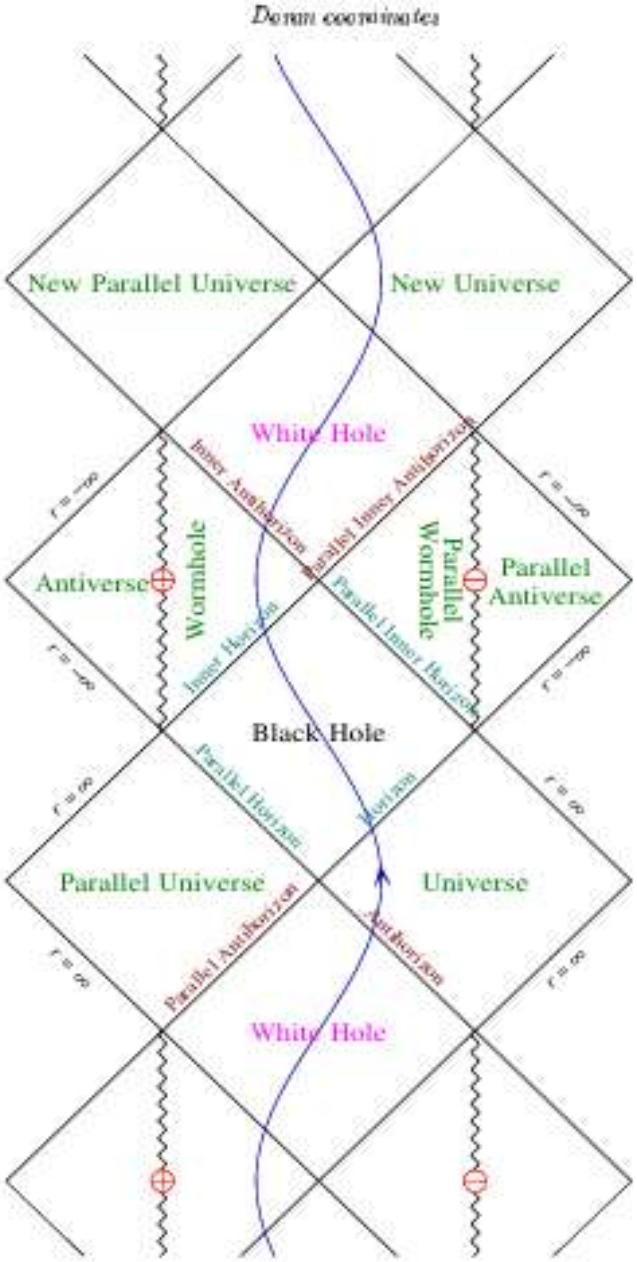

Figure 6. Penrose diagram of the Kerr-Newman geometry. The diagram is similar to that of the Reissner-Nordström geometry, except that it is possible to pass through the disk at r = 0 from the Wormhole region into the Antiverse region. This Penrose diagram, which represents a slice at fixed θ and ϕ, does not capture the full richness of the geometry, which contains closed time like curves in a torus around the ring singularity, the sisytube.

3. Modelling of a Black Hole

We are going to use the theory developed in the paper: Electrical-Quantum Modelling of the Neutron and Proton as a Three-Phase Alternating Current Electrical Generator. Determination of the Number of Quarks-Antiquarks-Gluons and Gravitons, Inside a Neutron, v2.

Let us remember the following, in the LHC particle accelerator, it has been successfully isolated antimatter, that is, matter with energy (-$\hbar\omega$).

We will also remember, when a black hole forms, a star of more than 25 solar masses explodes in a supernova and collapses due to gravity, giving rise to a black hole of approximately 3 solar

 doi:10.20944/preprints202408.0101.v1

masses. It is important to note that the star loses 22 solar masses to produce a black hole of 3 solar masses.

Let's also remember the following definition of a black hole:

A black hole is a plasma of quarks and gluons, a superfluid or a super-solid, which forms a high-temperature bosonic-fermionic condensate, characterized because the matter is in its state of maximum energy, that is, as a whole it behaves like an isolated quark.

This definition is in the paper: Rlc Electrical Modelling of Black Hole and Early Universe. Generalization of Boltzmann's Constant in Curved Space-Time.

In the definition of a black hole, we are going to highlight the word isolated quark, we could interpret this as meaning that inside a black hole there is no quarks - antiquarks - gluons interaction, only the quarks - gluons interaction exists.

With this we are proposing that inside a black hole there is no antimatter ($-\hbar\omega$), that is, the interior of a black hole is made up only of matter ($\hbar\omega$).

Recalling again that at the LHC it was possible to isolate antimatter, that is, matter ($-\hbar\omega$) and also remembering that to form a black hole a star of 25 solar masses explodes in a supernova and by gravitational collapse forms a black hole of 3 solar masses, we are wondering!!!!!!

Could it happen that the gravitational collapse process separates matter from anti-matter in analogy to what happens at the LHC?

The explosion of a supernova goes beyond chemical energy or nuclear energy; That is why we propose that a supernova when it explodes separates matter from antimatter, in other words, the black hole that remains would be made up of matter and the antimatter expands in the space-time that surrounds the black hole.

Let us remember that for temperatures greater than 10^{15} kelvin, the symmetry breaking of the electro-weak force occurs and consequently the separation of the electromagnetic force field and the weak force field; For higher temperatures, the interactions of the electromagnetic force field and those of weak force do not exist.

According to what is stated in the theory *RLC Electrical Modelling of Black Hole and Early Universe. Generalization of Boltzmann's Constant in Curved Space-Time*; a black hole has a temperature of 10^{13} K, that is, the supernova explosion to form a black hole produces a temperature higher than 10^{13} K, in this way, it is possible to reach at the temperature of symmetry breaking, which would mean that a black hole would form a high-temperature Bose-Einstein condensate, a single primordial atom.

Hypothesis: the disappearance of the interactions of the electromagnetic force field and the weak force field together with the gravitational collapse of a star of more than 25 solar masses due to the explosion of a supernova generates a black hole of mass ($\hbar\omega$), matter; that is, a black hole without antimatter, without mass ($-\hbar\omega$).

Taking the above into account, we are going to propose the following vector model of a black hole and we are going to compare it with the vector model of a neutron.

We compare it with a neutron because we assume that the net charge of a black hole is also zero.

NEUTRON											
		INTERACTION 1				INTERACTION 2					
R B G		R	B	G		R	R	B	B	G	G
D D U		D	D	U		D	D	D	D	U	U
D D U		D	D	U		D	U	D	U	D	D
R B G		R	B	G		B	G	R	G	R	B
m(Mev/c^2)	939.5	211.7				727.8					
		85.7	85.7	40.3		99	99	99	99	165.9	165.9

Figure 7. Neutron.

Preprints.org (www.preprints.org) | NOT PEER-REVIEWED | Posted: 2 August 2024 doi:10.20944/preprints202408.0101.v1

BLACK HOLE											
		INTERACCION 1				INTERACCION 2					
RBG		R	B	G		R	R	B	B	G	G
DDU		D	D	U		D	D	D	D	U	U
DDU		D	D	U		D	U	D	U	D	D
RBG		R	B	G		B	G	R	G	R	B

Figure 8. Equivalent Neutron / Black Hole.

We are going to carry out mathematical calculations to see if we can obtain important conclusions:

We will calculate the Schwarzschild´s radius for a black hole of 3 solar masses.

$M = 6\ 10^{30}$ kg

mn = 939.56 MeV/c^2

$mn = 1.675\ 10^{-27}$ kg

Where mn is mass of the neutron.

$Rs = 2GM / c^2$

$Rs = (2 \times 6.67\ 10^{-11} \times 6\ 10^{30}) / 9\ 10^{16} = 80.04\ 10^{19} / 9\ 10^{16}$

$Rs = 8.89\ 10^3$ m

Where Rs is Schwarzschild´s radius.

We will calculate the volume of a black hole of three solar masses:

$V = 4/3\ \pi\ R^3$

$V = 1.33 \times 3.14 \times (8.89\ 10^3)^3$

$V = 1.33 \times 3.14 \times 702.59\ 10^9$

$V = 2934.15\ 10^9$

Where V is volume of the black hole.

We will calculate the volume of a neutron.

$Rn = 0.4\ 10^{-15}$ m

Where Rn is radius of the neutron.

$Vn = 4/3\ \pi\ R^3$

$Vn = 4/3\ \pi\ R^3 = 4/3 \times 3.14 \times (0.4\ 10^{-15})^3 = 0.267\ 10^{-45}\ m^3$, volume of the neutron.

$Vn = 0.267\ 10^{-45}\ m^3$,

Where Vn is volume of the neutron.

We will define D, a scale factor that represents the ratio of the volume of a black hole of 3 solar masses to the volume of the neutron.

D = V / Vn

Where D is scale factor.

D = V / Vn

$D = V / Vn = 2934.15\ 10^9 / 0.267\ 10^{-45} = 10989.34\ 10^{54}$

$D = 10.98\ 10^{57}$

We divide the mass of the black hole by the factor D.

Mn = M/D

$Mn = 6\ 10^{30}$ kg / $10.98\ 10^{57}$ kg

$Mn = 0.54\ 10^{-27}$ kg

If we divide Mn by mn, we obtain:

$K = Mn / mn = 0.54\ 10^{-27} / 1.67\ 10^{-27} = 0.32$

K = 0.32

Mn = 939.56 x 0.32 = 300.65 MeV/c

Mn = 300.65 MeV/c

Where Mn is the mass contained in a black hole, in a volume equivalent to that of the neutron.

This result that we obtained for Mn is very interesting, it is telling us that the mass content in a volume equivalent to that of a neutron inside a black hole is less than the mass of the neutron; precisely this coincides with our assumption that inside a black hole we do not have antimatter, a black hole is formed only by matter.

 doi:10.20944/preprints202408.0101.v1

If the statement is true: a black hole is formed only by matter, the antimatter is expelled when the collapse of a star occurs and a supernova explosion occurs; This would explain the enigma of antimatter during the Big Bang, it would explain why the Big Bang produces a universe of matter and not antimatter.

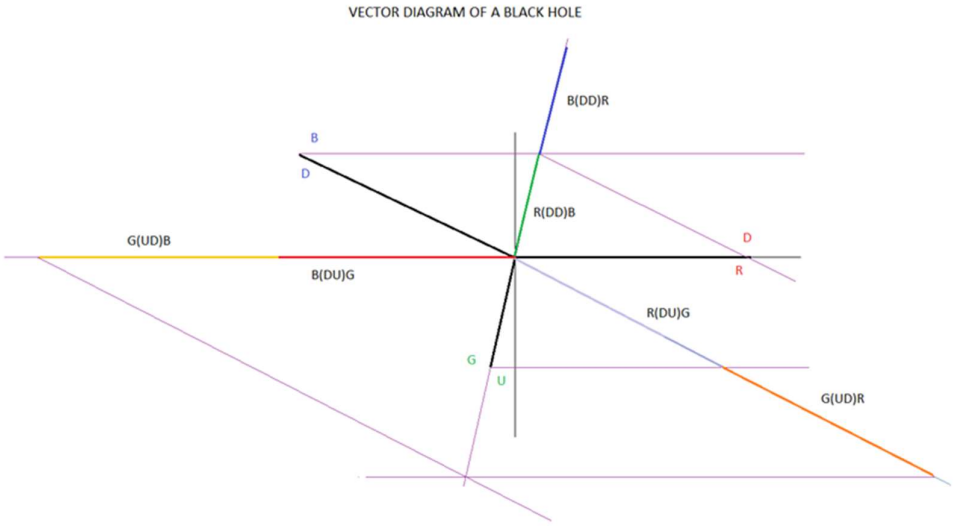

Figure 9. Vector Diagram of a Black Hole.

Considering the conversion factor, we calculate the value of interaction 2, for the six corresponding dipoles, which we will represent below:

R(DD)B = 28.54 MeV/c²
R(DU)G = 60.88 MeV/c²
B(DD)R = 28.54 MeV/c²
B(DU)G = 60.88 MeV/c²
G(UD)R = 60.88 MeV/c²
G(UD)B = 60.88 MeV/c²

We are going to represent these values in Figure 10:

BLACK HOLE												
		INTERACTION 1				INTERACTION 2						
RBG		R	B	G		R	R	B	B	G	G	
DDU		D	D	U		D	D	D	D	U	U	
DDU		D	D	U		D	U	D	U	D	D	
RBG		R	B	G		B	G	R	G	R	B	
m(Mev/c^2)	300.60	0				300.60						
		0	0	0		28.54	60.88	28.54	60.88	60.88	60.88	

Figure 10. Equivalent Neutron/ Black Hole.

In Figure 10, we see that the equivalent mass of the neutron inside a black hole is approximately one-third of the mass of the neutron.

We observe that the direct interaction, interaction 1, is null.

We observe that the cross interaction, interaction 2, the scalar sum is equal to 300.60 MeV/c² and the vector sum is zero

Now we are going to present the graphic representation of the electrical model in Figure 10:

 doi:10.20944/preprints202408.0101.v1

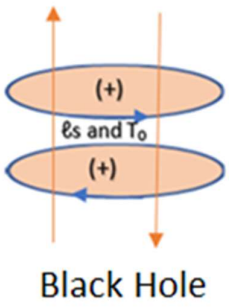

Figure 11. Electrical modelling of a black hole.

Next, using Figure 11 and 12, we are going to make a brief description of the internal behaviour of a black hole.

Before starting our description, let us remember that in our RLC electrical model, a black hole is represented by:

Here we put forward the hypothesis of a black hole growth in analogy to an RC electrical circuit that grows according to a constant Tau being defined as:

$$\tau = RC \qquad (40)$$

First, we will consider the total mass of a black hole to consist of the sum of baryonic mass and dark matter mass (equation 41), considering dark matter as an imaginary number.

$$M = m - i\delta \qquad (41)$$

Where M is the total mass of a black hole, m is the baryonic mass; δ corresponds to dark matter and I is the irrational number $\sqrt{-1}$. This equation is in analogy to impedance of an RC circuit.

$$Z = R - iX_c \qquad (42)$$

Where z represents impedance; R represents resistance and Xc represents reactance.

If proper accelerations for the masses are introduced in equation (41) we obtain the following:

$$F = f - i\varphi \qquad (43)$$

Where F is the total force, f is the force associated to baryonic mass, and $i\varphi$ is the force associated to dark mass. In analogy to a phasor diagram for an RC circuit, in which the reactance phasor lags the resistance phasor R by $\frac{\pi}{2}$, we can represent the two forces associated to barionic matter and dark matter as two orthogonal vectors (Figure 12).

Vector diagram of forces in a black hole for circular motion with constant acceleration:

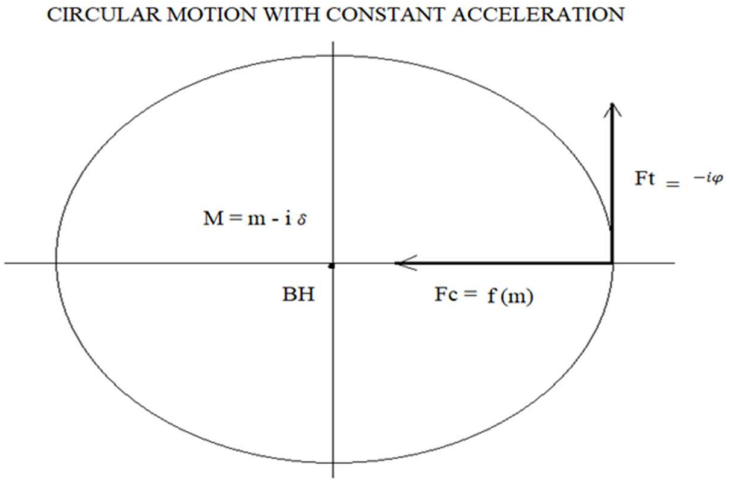

Figure 12. Vector representation of the forces in a black hole. Fc = f, represents the force towards the interior of the black hole generated by the mass m and Ft = -iφ, is a tangential force that retards Fc by 90 degrees, generated by the mass δ.

 doi:10.20944/preprints202408.0101.v1

taking into account Newton's equation of universal gravitation:

$$F = - (G\ M1\ M2)/r^2$$

The sign (-) of the equation means that the force Fc is at 180 degrees with respect to the resistance R and the force Ft is also at 180 degrees from the reactance Xc.

It is important to make clear the physical interpretation of the imaginary mass, it is simply telling us that the force Ft due to the mass δ lag the force fc by 90 degrees, that lag is represented by the imaginary number i. Later we will determine that the mass δ, is the result of v > c inside a black hole.

Where v is the speed of a massless particle and c is the speed of light in a vacuum.

Figure 12 is represented for a circular motion with constant acceleration simply because the tangential velocity of a particle is proportional to the radius from the centre of the black hole multiplied by the average angular frequency.

$$Vt = r\ \omega$$

The contribution of (Ft, Vt) is what makes the speed of the galaxy remain constant as the radius of the galaxy grows.

Where Vt represents the tangential velocity of a galaxy, r is the radius from the galaxy, and ω is the average angular velocity of the rotation of the galaxy.

Circular motion with constant acceleration tells us that the mass input into a black hole is negligible with respect to the black hole's own mass.

The growth of a black hole according to the tau constant is an intrinsic property of a black hole and is independent of the amount of matter that enters a black hole.

To calculate the total energy associated to the black hole, we can introduce its total mass (equation 41) into:

$$E^2 = c^2p^2 + c^4M^2 \qquad (44)$$

Where E is energy; c represents the speed of light and m represents the mass. This lead to:

$$E^2 = c^2p^2 + (m^2 - \delta^2)c^4 - 2im\delta c^4. \qquad (45)$$

We can assume that during the big bang inflation phase baryonic matter was overrepresented compared to dark matter together with an infinitesimal momentum, which would give us from equation (76) the following:

$$E^2 = -\delta^2c^4 \quad ; \quad E = (+/-)\delta c^2 i \qquad (46)$$

As expected, this result corresponds to the total energy of the universe at the big bang if we consider it to be made of dark matter represented as a reactance in an RC circuit.

The positive value of E is determined by matter, there is no antimatter inside a black hole.

If we consider charge as a fundamental property of matter, $E = (+)\delta c^2 i$, represents the amount of relativistic dark matter inside the black hole at the time of disintegration.

If we consider mass as a fundamental property of matter, $E = (-)\delta c^2 i$, represents the amount of relativistic dark matter inside a black hole, which exerts a repulsive gravitational force at the moment of disintegration. This repulsive gravitational force is what generates the dark energy after the Big Bang.

At time T0, when the black hole disintegrates and the Big Bang occurs, roughly all matter was dark matter, relativistic dark matter.

We could also consider a universe at infinity proper time in which baryonic matter is dominant over dark matter, which would transform equation (45) back into equation (44) but with baryonic matter.

$$E^2 = c^2p^2 + m^2c^4. \qquad (47)$$

We are also going to remember, the collapse of a star to form a black hole, separates the matter from the antimatter, the matter remains inside the black hole and the antimatter is expelled to the outside of the black hole, that is, into space-time.

This is telling us that the vacuum inside a black hole is less dense than the vacuum outside. We call the vacuum inside a black hole true vacuum and the vacuum outside a black hole (space-time) we call it meta-stable vacuum.

If we look at it from the point of view of the density of virtual particles, the density of virtual particles inside a black hole is lower than the density of virtual particles outside a black hole. Therefore, inside black hole, a particle like the photon could travel at a speed v > c, this allows us to state again, as the difference of v with respect to c increases, the Planck length decreases. Inside a

 doi:10.20944/preprints202408.0101.v1

black hole, the gravitational Planck length Lpɢ decreases with respect to the electromagnetic Planck length Lpε.

The decrease in Lpɢ with respect to Lpε is not linear like that of a shock absorber, it is similar to the movement of a corkscrew, precisely that is what generates the torsional or tangential force. This tangential force is what makes the black hole rotate counter clockwise.

This model resembles a Kerr black hole, dynamic and rotating, with a singularity inside in the form of a spiral/coil or ring, ring singularity. See Figure 13.

Everything we have stated was analysed in the paper: RLC Electrical Modelling of Black Hole and Early Universe. Generalization of Boltzmann's Constant in Curved Space-Time.

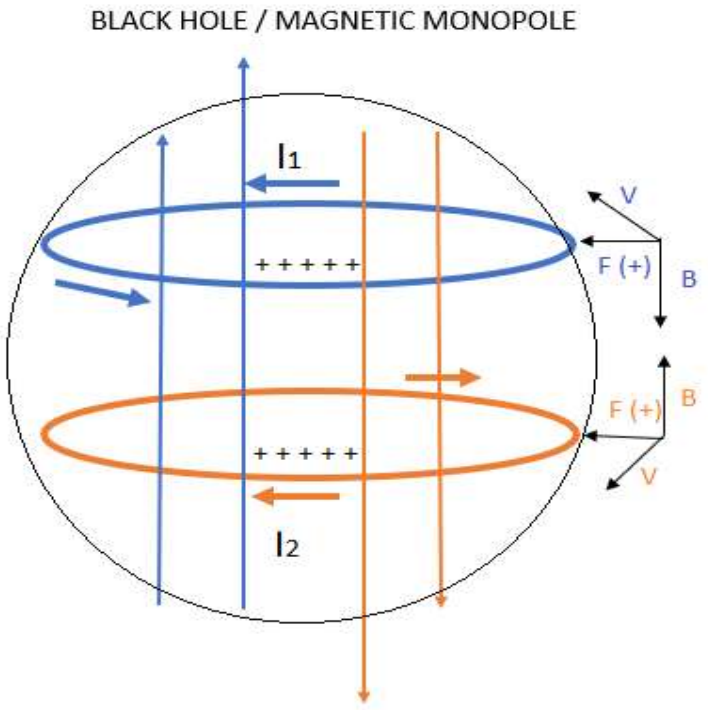

Figure 13. Diagram of the black hole model.

If we look at Figure 13, we see that the black hole is divided into two parts, an upper hemisphere and a lower hemisphere.

The dynamics of the upper hemisphere is dominated by bosonic particles that rotate counter clockwise, these particles resemble a ring or coil, which we represent by the current I_1.

If we consider the right-hand rule, the current I_1 generates a magnetic field B that goes up inside the coil (upper hemisphere) and goes down outside the coil, as shown in Figure 13.

The dynamics of the lower hemisphere is dominated by bosonic particles that rotate in a clockwise direction, these particles resemble a ring or coil, which we represent by the current I_2.

If we consider the right-hand rule, the current I_2 generates a magnetic field B that flows downwards inside the coil (lower hemisphere) and rises outside the coil, as shown in Figure 13.

If we take an infinitesimal part of the upper and lower coil, we can assume that they behave like two parallel wires in which the current is in the opposite direction, in this case the force generated between the two wires whose current is in the opposite direction is a force of repulsion. Both coils generate repulsive forces between each other.

If we look at Figure 13; the electric current I_1 with a positive charge moves counter clockwise, now if we look at the electric current I_2 with positive charges it moves clockwise; In other words, the electric field between the upper and lower coils generates a repulsion force between the upper coil and the lower coil.

 doi:10.20944/preprints202408.0101.v1

In other words, there is a magnetic field B, which generates a force that causes the upper coils and the lower coil to repel each other, and there is an electric field E, which generates a force between the upper coil and the lower coil that causes both coils also repel each other.

The repulsion forces between the upper hemisphere coil and the lower hemisphere coil, generated by the magnetic and electric fields, are counteracted by the gravitational force towards the interior of the black hole.

Again, if we look at Figure 13, there is an equatorial zone of the black hole between the upper and lower coil in which the magnetic field and the electric field are not defined. It is an indeterminate region, a turning point.

If we analyse the magnetic fields outside the black hole, at the height of the upper coil, we observe that the magnetic field has a downward direction, if we consider a particle with a positive charge, we see that the magnetic field B generates a force towards the interior of the black hole. see Figure 13.

If we analyse the magnetic fields outside the black hole, at the height of the lower coil, we observe that the magnetic field has an upward direction, if we consider a particle with a positive charge, we see that the magnetic field B generates a force inward of the black hole. see Figure 13.

This mechanism, recently described, tells us that the magnetic field that surrounds the black hole at the equator generates a force that causes positively charged particles to move towards the interior of the black hole and negatively charged particles are repelled, moving away from the black hole.

If we consider Hawking radiation, which tells us that a pair of particles of matter ($\hbar\omega$) and antimatter ($-\hbar\omega$) are produced in the event horizon of a black hole, it is assumed that the matter particles ($\hbar\omega$) fall into a black hole and antimatter ($-\hbar\omega$) are repelled out of a black hole. However, the magnetic field B outside a black hole at the height of the equator tells us that the particles with a positive charge of matter ($\hbar\omega$) and antimatter ($-\hbar\omega$) are those that fall into the interior of a black hole and the particles with a negative charge of matter ($\hbar\omega$) and antimatter ($-\hbar\omega$), are repelled and move away from the black hole.

The statement is very important, it is telling us, the interior of a black hole is made up only of positive charges.

Inside a black hole, in the domain of gravitational force, there are only positively charged bosonic particles which behave like a Bose-Einstein condensate. The black hole becomes a giant atom with a positive charge and its event horizon indicates the limit of the gravitational envelope that encloses the bosonic particles with positive charges.

Let us remember that from the scalar point of view, the black hole is made up of positive particles, but if we consider it from the vector point of view, the net charge resulting from a black hole is zero.

If we consider the magnetic field outside the black hole between the two coils, strong enough to generate pairs of particles and antiparticles in a vacuum, we can affirm that this mechanism would be powerful enough to produce an accretion disk around the equator of the black hole, which the black hole would use to feed on particles and grow. The black hole is self-sustaining, it feeds itself and is not dependent on devouring stars and other bodies to grow.

If we look at the upper hemisphere, above the upper coil there is an area in which the dynamics become dominated by the magnetic field B in an upward direction. The same thing happens with the lower hemisphere, from a certain distance, the dynamics become dominated by the magnetic field B in the lower direction. An example of what is stated is a quasar.

4. Application of the Model And Results

We are going to make a correlation, a parallelism between the theory that describes a Kerr-Newman black hole with the theories of the following papers: *RLC Electrical Modelling of Black Hole and Early Universe. Generalization of Boltzmann's Constant in Curved Space-Time*, and *Electrical-Quantum Modelling of the Neutron and Proton as a Three-Phase Alternating Current Electrical Generator. Determination of the Number of Quarks-Antiquarks-Gluons and Gravitons, Inside a Neutron*. We will use these theories to analyse the behaviour of our model.

4.1. Correlation between Kerr-Newman Black Hole vs. RLC Electrical Modelling of a Black Hole

1. We are going to perform an analysis for the condition: $M^2 > Q^2 + a^2$

Preprints.org (www.preprints.org) | NOT PEER-REVIEWED | Posted: 2 August 2024 doi:10.20944/preprints202408.0101.v1

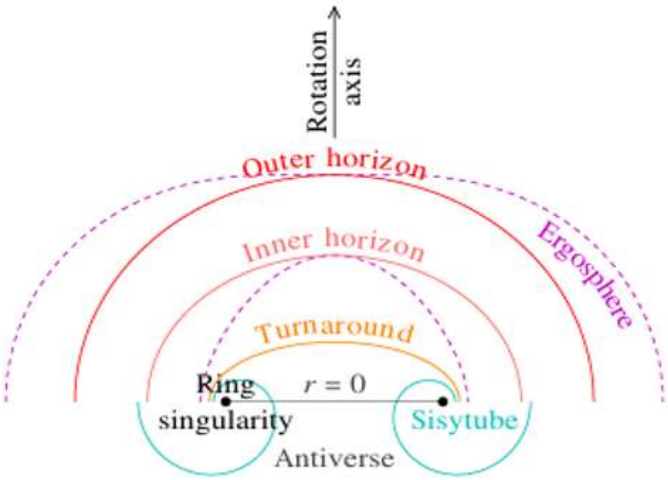

Figure 14. Spatial geometry of a Kerr-Newman black hole with charge Q = 08M and spin parameter a = 056M. The lower half shows r ≤ 0, the Antiverse. The outer and inner horizons are confocal oblate spheroids whose focus is the ring singularity. The Sisytube is a torus enclosing the ring singularity, that contains closed time like curves.

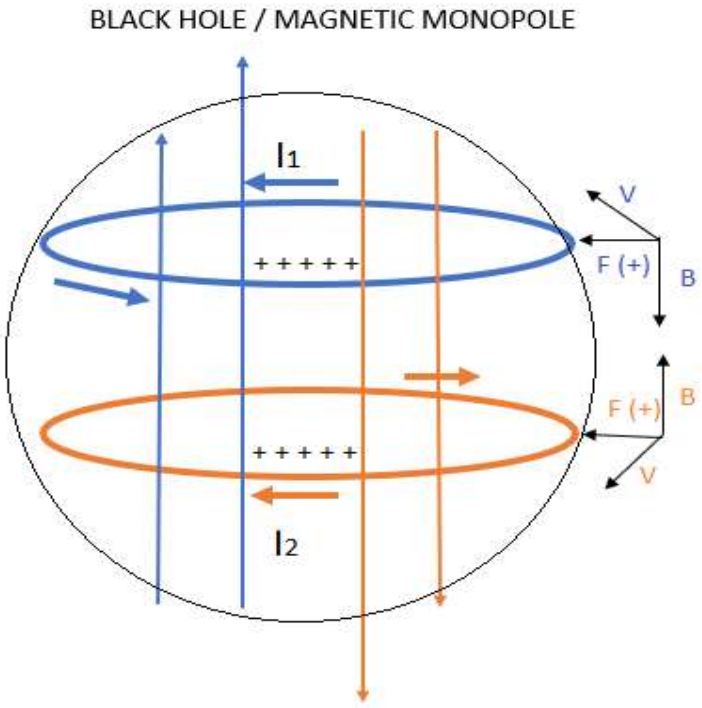

Figure 15. Diagram of the black hole model.

If we observe and compare Figures 14 and 15, we see the following:

In both models the black holes rotate around their axial axis.

In Figure 14, we can see an ergosphere, an outer horizon and an inner horizon. We also observe that the outer and inner horizons are cofocal oblate spheroids whose focus is the ring singularity.

$$\boxed{r_{\pm} = M \pm \sqrt{M^2 - Q^2 - a^2}} \ .$$

In Figure 15, we can also observe an event horizon and a ring singularity, we can assume that the event horizon is cofocal oblate spheroids and whose focus is the ring singularity.

Preprints.org (www.preprints.org) | NOT PEER-REVIEWED | Posted: 2 August 2024 doi:10.20944/preprints202408.0101.v1

Under this condition, $M^2 > Q^2 + a^2$; The black hole is born and grows, we can say that it represents the first moments of the life time of a black hole.

As the black hole grows, the distance between the outer horizon and the inner horizon decreases.

The particles that enter the black hole pass through the ergosphere, cross the outer horizon and the inner horizon and finally fall into the ring singularity. Inside the ring singularity ($r \leq 0$) the bosonic particles move at a speed greater than the speed of light, which generates an additional mass which we represent in our model as $-i\delta$ *(see equation 41)*. This additional mass generates a gravitational force that is not attractive and is the gravitational force that gives rise to dark matter.

Let us remember that a black hole grows in the same way as the Tau constant of an RC circuit (equation 40).

We are going to represent the graphs and calculations that describe the growth of a black hole, the complete mathematical development can be found in the paper: *RLC Electrical Modelling of Black Hole and Early Universe. Generalization of the Boltzmann constant in curved spacetime.*

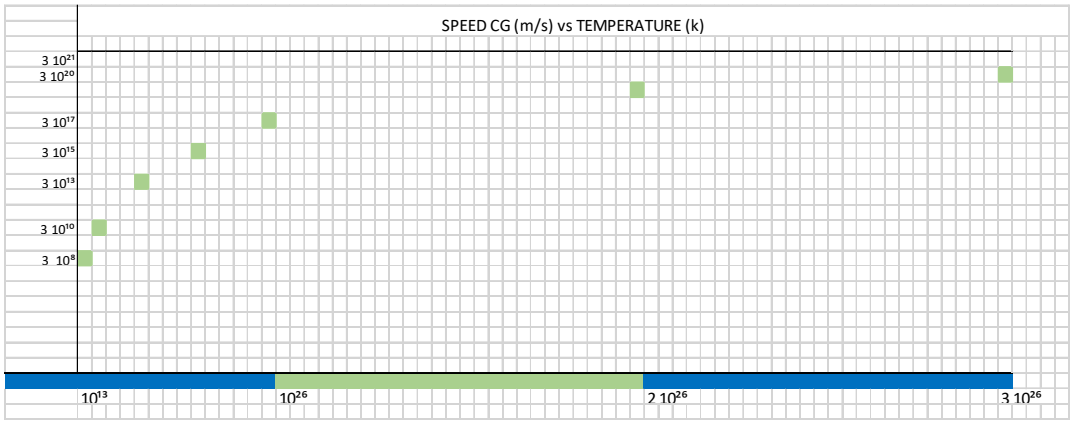

Figure 16. Represents the variation of speed C_G, as a function of temperature T, inside a black hole.

Now we are going to present the Penrose Diagram:

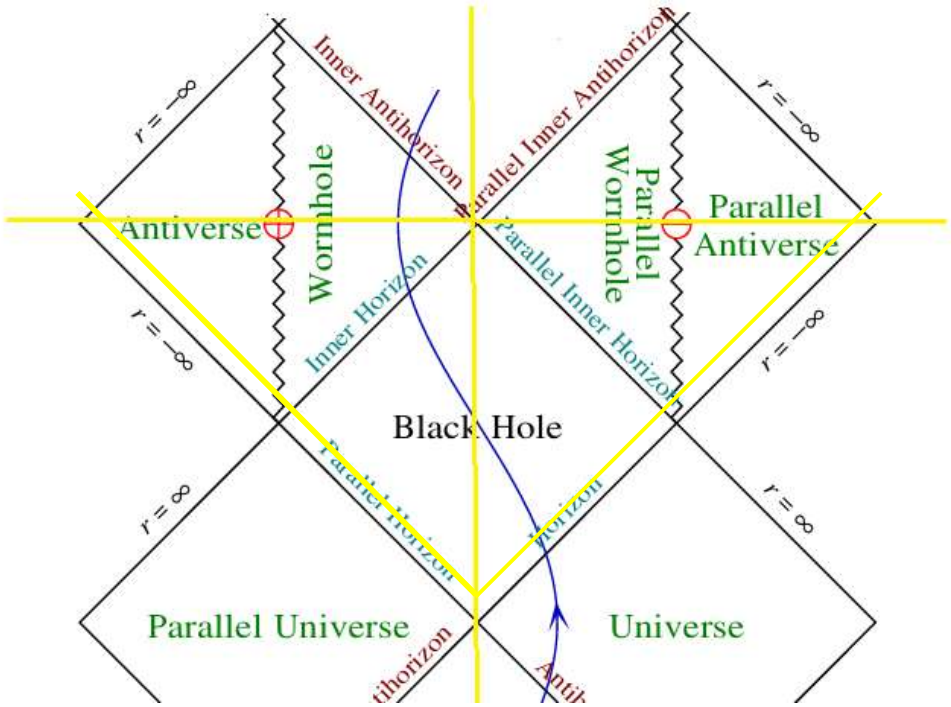

Figure 17. Penrose diagram of the Kerr-Newman geometry, $M^2 > Q^2 + a^2$.

 doi:10.20944/preprints202408.0101.v1

Now we are going to try to relate Figure 15 with Figure 17.

If we look at Figure 15, we see that the spheroid that represents a black hole can be divided into two parts, an upper part and a lower part.

If we look at Figure 17, if we consider the yellow vertical line, we can also divide the graph into two parts, a spatial part representing the right side and a spatial part representing the left side.

If we consider a test particle, we see in Figure 15 that it can enter the upper part, at the equator of the spheroid, cross the event horizon and head to the upper singularity. There is also another option in which the test particle could enter the lower part of the equator, in the spheroid, cross the event horizon and head to the lower singularity.

If we consider a test particle, we see in Figure 17, in analogy with Figure 15, that it can enter the left side of the black hole, in the ergosphere, cross the event horizon, pass through the wormhole region and end up in the antiverse region. There is also another option in which the test particle could enter on the right side of the black hole, in the ergosphere, cross the event horizon, cross the parallel wormhole region and end up in the parallel antiverse region.

If we look at Figure 15, both currents I_1 and I_2 have a positive charge and move in the opposite direction. We observe that current I_1 moves counter clockwise and generates an upward magnetic field (blue); Current I_2 moves clockwise and generates a downward magnetic field (orange).

Both the electric and magnetic force generated by currents I_1 and I_2 produce a repulsion force between the coils, this is counteracted only by the gravitational force.

If we look at Figure 17, if we consider a test particle, we see that there is a repulsion force between the left side of the graph and the right side, for example, if a test particle (1) that enters the black hole, enters the ergosphere, enter the wormhole and antiverse; If we consider Figure 15, by analogy the particle heads upward until it reaches the ring singularity. Now we consider the test particle (2) that enters the black hole, ergosphere, parallel wormhole, parallel antiverse, by analogy to Figure 15, the test particle heads downward until it reaches the ring singularity. The test particle (1) is directed upward, while the test particle (2) is directed downward, as if both positive particles were under opposite forces.

There is an analogy between graph 15 and graph 17, the upper part of graph 15, from the equator up, corresponds to the left symmetrical region of the vertical yellow line of graph 17; The lower part of graph 15, from the equator downwards, corresponds to the right symmetrical part of the vertical yellow line of graph 17.

Another important analogy that we must highlight is the ring singularity, above the equator in Figure 15, which corresponds to the antiverse in the left symmetry of graph 17; We must also highlight the ring singularity below the equator in Figure 15, which corresponds to the parallel antiverse in the right symmetry of graph 17.

Finally, it is important to note that the black hole grows and as it increases in size, the regions of the black hole that we call ergosphere, wormhole (parallel wormole) and antiverse (parallel antiverse) also grow.

Here, it is important to note that although the black hole grows, nothing material comes out of the black hole, therefore we can represent this in Figure 17 only with the yellow triangle. What is stated here is very important.

2. We are going to perform an analysis for the condition: $\boldsymbol{M^2 = Q^2 + a^2}$

The Kerr-Newman geometry is called extremal when the outer and inner horizons coincide:

$$r_+ = r_-,$$

We see that in this condition there is a single event horizon, which we are going to represent in the following Figure:

 doi:10.20944/preprints202408.0101.v1

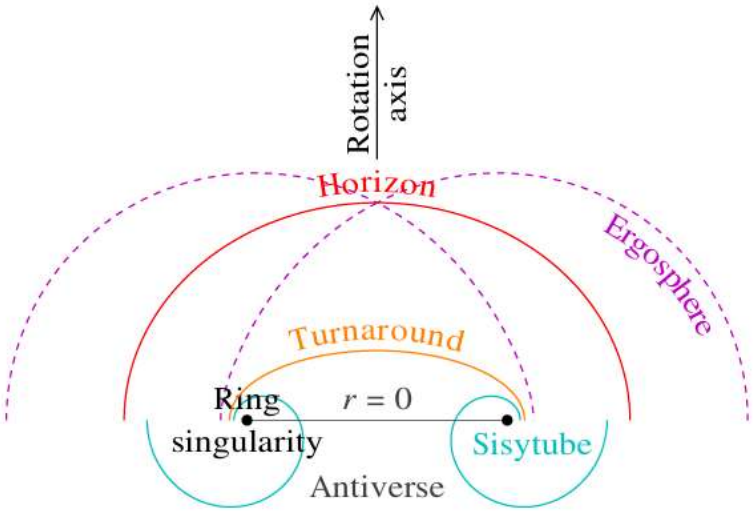

Figure 18 Spatial geometry of an extremal Kerr-Newman black hole with charge Q = 08M and spin parameter a = 06M.

We could express the relationship $M^2 = Q^2 + a^2$ in another way:

$M^2 / (Q^2 + a^2) = 1$

This is telling us that the growth of a black hole has a limit, that the amount of matter it devours is limited and if it exceeds that limit it has to be expelled in some way; Therefore, the amount of matter that enters the interior of the ring singularity (antiverse) is limited by the mass M of the black hole.

For example, we could assume that this limit is generally exceeded when a stellar black hole devours a star, a quasar.

Here, it is important to note that although the black hole grows, nothing material comes out of the black hole, therefore we can represent this in Figure 17 only with the yellow triangle.

3. We are going to perform an analysis for the condition: $M^2 < Q^2 + a^2$

We could express the relationship $M^2 < Q^2 + a^2$ in another way:

$M^2 / (Q^2 + a^2) < 1$

In this condition, the event horizon disappears and we say that we have a naked singularity.

In this condition, we can observe that the amount of matter (charge) that the black hole devours exceeds its mass.

We said that the growth of a black hole is limited by its mass M, therefore, the amount of matter that enters a black hole is limited by the mass M, that is, if the black hole devours a greater amount of matter that its mass M, then somehow the black hole has to eliminate the excess matter it is ingesting.

We are going to represent the statement in the following Figure:

Preprints.org (www.preprints.org) | NOT PEER-REVIEWED | Posted: 2 August 2024 doi:10.20944/preprints202408.0101.v1

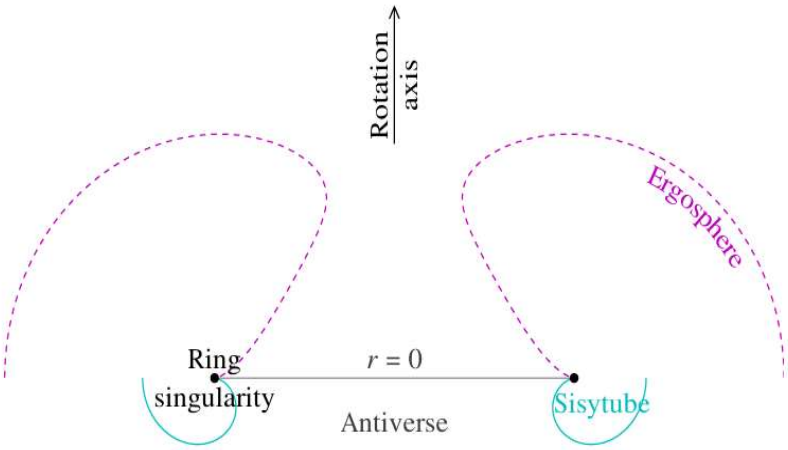

Figure 19. - Spatial geometry of a super-extremal Kerr black hole with spin parameter a = 104M. A super-extremal black hole has no horizons.

Let's interpret what we said in a Penrose diagram.

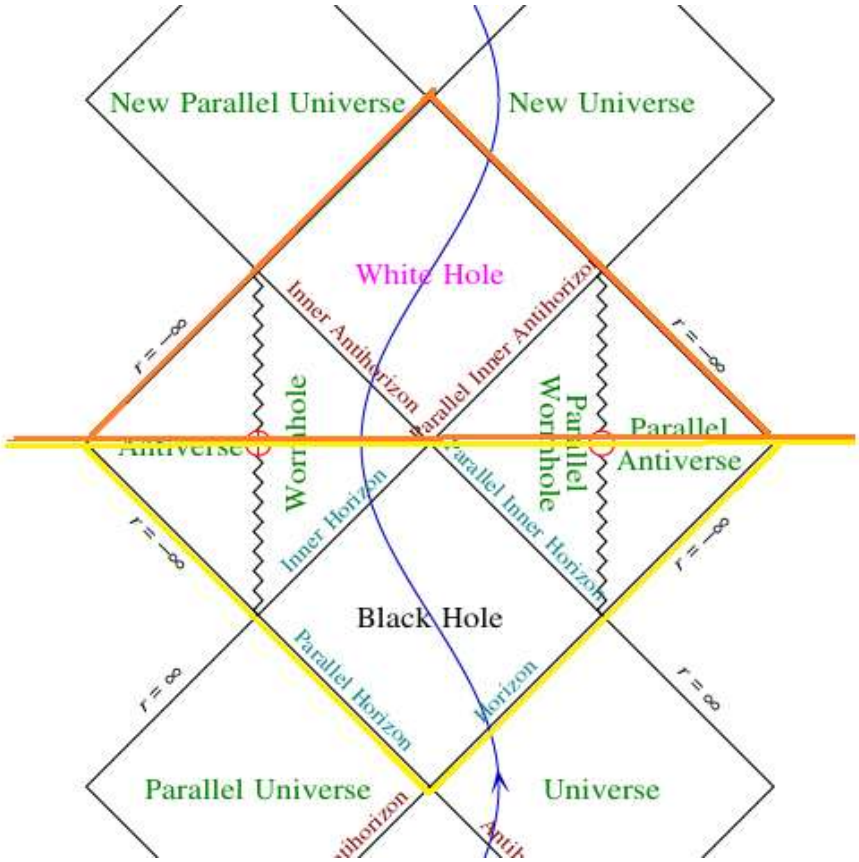

Figure 20. - Penrose diagram of the Kerr-Newman geometry, $M^2 < Q^2 + a^2$.

Figure 20, Let's consider two sets of test particles, the two sets of test particles enter the black hole (ergosphere), one set through the horizon and the other set through the parallel horizon; Now let's look at Figure 15, one set of test particles enters above the equator of the spheroid and the other set of particles enters below the equator of the spheroid.

Let us remember that we are under the condition: $M^2 < Q^2 + a^2$

Figure 20, the first set that was in the parallel universe, enters the black hole (ergosphere) through the parallel horizon, part of that set of particles is devoured by the black hole and ends up

 doi:10.20944/preprints202408.0101.v1

in the antiverse and the rest of the particles leave the black hole, crosses the inner antihorizon and ends in the new parallel universe. The second set of particles follows a similar path, it enters the black hole (ergosphere) through the horizon, part of that set of particles is devoured by the black hole and ends up in the parallel antiverse and the rest of the particles leave the black hole. It crosses the parallel inner antihorizon and ends in the new universe.

If we look at Figure 15, the first set of particles enters the black hole above the equator of the spheroid, part of the set of particles is devoured by the black hole and goes to the ring singularity and the rest of the particles are expelled out of the black hole, upwards. Similarly, the second set of particles enters the black hole through the lower part of the equator of the spheroid, part of the set of particles is devoured by the black hole and goes to the ring singularity and the rest of the particles are expelled from the hole black, down.

If we compare Figure 17 with Figure 20, we see that there is a difference between them.

Figure 17 represents a black hole that grows, under the condition $M^2 \geq Q^2 + a^2$, which is telling us that no matter comes out of the black hole. This is represented by the inverted yellow triangle.

Figure 20 represents a black hole that grows and has an associated relativistic jet, under the condition $M^2 < Q^2 + a^2$, which is telling us that part of the matter that the black hole devours is expelled. This is represented by the two highlighted triangles; the yellow triangle representing the black hole devouring matter and the orange triangle (white hole) representing the amount of matter ejected from the black hole.

An example of the true meaning of what Figure 20 represents would be a quasar.

Reissner-Nordström Black Hole, the inflationary instability, under the condition Q > M, at point X, an inflationary instability occurs that produces feedback which generates the relativistic jets. The interior mass is not the only thing that increases exponentially during mass inflation. The proper density and pressure, and the Weyl scalar (all gauge-invariant scalars) exponentiate together.

This is analogous to what happens in a black hole with the Kerr-Newman geometry, part of the mass that enters the black hole ends up in the antiverse (ring singularity) and the rest of the mass is ejected in the form of a relativistic jet, is given for the condition $M^2 < Q^2 + a^2$.

Under this interpretation, the universe, the parallel universe, the new universe and the new parallel universe actually represent our only universe. See Figure 20.

Under this interpretation, the antiverse and the parallel antiverse in Figure 17 and 20, represent in Figure 15, the ring singularity that is at the top of the equator of the spheroid and the ring singularity that is at the bottom of the equator of the spheroid.

According to our description, the black hole model in Figure 15 perfectly emulates the black hole model represented in Figure 20, corresponding Penrose diagram of the Kerr-Newman geometry.

4. We are going to perform an analysis for the condition: $M = Mc$

Here, we are going to analyse the condition in which the black hole reaches its critical mass Mc.

In the theory of the paper*: RLC Electrical Modelling of Black Hole and Early Universe. Generalization of Boltzmann's Constant in Curved Space-Time*; we put forward the hypothesis of a black hole growth in analogy to an RC electrical circuit that grows according to a constant Tau being defined as:

$$\tau = RC \qquad (48)$$

In a capacitor when its charge reaches the value of 5τ, we say that the capacitor reached its maximum charge, in analogy to the capacitor, when the black hole reaches the value of 5τ it reaches its maximum mass value; Let us remember that a capacitor stores electrical energy and a black hole stores gravitational potential energy.

Let us remember that the mass of a black hole in the theory of the paper: *Rlc Electrical Modelling of Black Hole and Early Universe. Generalization of Boltzmann's Constant in Curved Space-Time*; It is represented by the following equation:

$$M = m - i\delta \qquad (49)$$

Where M is the total mass of a black hole, m is the baryonic mass; δ corresponds to dark matter and (i) is the irrational number $\sqrt{-1}$. This equation is in analogy to impedance of an RC circuit.

To calculate the total energy associated to the black hole, we can introduce its total mass (equation 49) into:

$$E^2 = c^2p^2 + c^4M^2 \qquad (50)$$

Where E is energy; c represents the speed of light and m represents the mass. This lead to:

 doi:10.20944/preprints202408.0101.v1

$$E^2 = c^2p^2 + (m^2 - \delta^2)c^4 - 2im\delta c^4. \qquad (51)$$

We can assume that during the big bang inflation phase baryonic matter was overrepresented compared to dark matter together with an infinitesimal momentum, which would give us from equation (51) the following:

$$E^2 = -\delta^2 c^4 \quad ; \quad E = (+/-)\delta c^2 i \qquad (52)$$

As expected, this result corresponds to the total energy of the universe at the big bang if we consider it to be made of dark matter represented as a reactance in an RC circuit.

The positive value of E is determined by matter, there is no antimatter inside a black hole.

If we consider charge as a fundamental property of matter, $E = (+)\delta c^2 i$, represents the amount of relativistic dark matter inside the black hole at the time of disintegration.

If we consider mass as a fundamental property of matter, $E = (-)\delta c^2 i$, represents the amount of relativistic dark matter inside a black hole, which exerts a repulsive gravitational force at the moment of disintegration. This repulsive gravitational force is what generates the cosmic inflation and dark energy after the Big Bang.

At time T0, when the black hole disintegrates and the Big Bang occurs, roughly all matter was dark matter. Relativistic dark matter.

We could also consider a universe at infinity proper time in which baryonic matter is dominant over dark matter, which would transform equation (51) back into equation (50) but with baryonic matter.

$$E^2 = c^2p^2 + m^2c^4. \qquad (53)$$

Here we put forward the hypothesis that the big bang is the convolution of the energy released by disintegration of the black hole with the space-time surrounding the black hole, being defined as:

$$(m - i\delta) * \mathcal{E} \qquad (54)$$

Where $m - i\delta$, is the total mass of a black hole, $\mathcal{E}$ is the space-time surrounding the black hole and * is the convolution symbol.

Equation (54) can be simplified and considered analogous to an RLC circuit.

Where RC represents a black hole and L represents the space-time around a black hole.

$$RC = m - i\delta \qquad (55)$$

$$L = \mathcal{E} \qquad (56)$$

the resolution of the quadratic equation of the RLC circuit will determine how space-time will expand after the Big Bang and the bandwidth of the equation will give us the spectrum of gravitational waves that originated during the Big Bang.

The growth of the black hole from its birth until it reaches the value of 5τ is represented in Table 2 and Figure 16.

Table 2. Represents values of ImI, baryonic mass; IδI, dark matter mass; IMI, mass of baryonic matter plus the mass of dark matter; IEmI, energy of baryonic matter; IEδI, dark matter energy; IEI, Sum of the energy of baryonic matter plus the energy of dark matter and Rs, Schwarzschild´s radius, as a function of, c, speed of light; C_G, speed greater than the speed of light; T, temperature in Kelvin; using the parametric equations.

Item	T	CG	C	I m I	I δ I	I M I	I Em I	I Eδ I	I E I	Rs
0	kelvin	m/s	m/s	kg	kg	kg	Joule	Joule	Joule	m
1	10^{13}	$3\ 10^{8}$	$3\ 10^{8}$	$6.00\ 10^{30}$	0	$6.00\ 10^{30}$	$5.40\ 10^{47}$	0	$5.40\ 10^{47}$	$8.89\ 10^{3}$
2	10^{14}	$3\ 10^{10}$	$3\ 10^{8}$	$6.00\ 10^{35}$	$6.00\ 10^{39}$	$6.00\ 10^{39}$	$5.40\ 10^{52}$	$5.40\ 10^{56}$	$5.40\ 10^{56}$	$8.89\ 10^{8}$
3	10^{17}	$3\ 10^{13}$	$3\ 10^{8}$	$6.00\ 10^{41}$	$6.00\ 10^{51}$	$6.00\ 10^{51}$	$5.40\ 10^{58}$	$5.40\ 10^{68}$	$5.40\ 10^{68}$	$8.89\ 10^{14}$
4	10^{21}	$3\ 10^{15}$	$3\ 10^{8}$	$6.00\ 10^{43}$	$6.00\ 10^{57}$	$6.00\ 10^{57}$	$5.40\ 10^{60}$	$5.40\ 10^{74}$	$5.40\ 10^{74}$	$8.89\ 10^{16}$
5	$1\ 10^{26}$	$3\ 10^{17}$	$3\ 10^{8}$	$6.00\ 10^{44}$	$6.00\ 10^{62}$	$6.00\ 10^{62}$	$5.40\ 10^{61}$	$5.40\ 10^{79}$	$5.40\ 10^{79}$	$8.89\ 10^{17}$
6	$2\ 10^{26}$	$3\ 10^{18}$	$3\ 10^{8}$	$3.00\ 10^{47}$	$3.00\ 10^{67}$	$3.00\ 10^{67}$	$2.70\ 10^{64}$	$2.70\ 10^{84}$	$2.70\ 10^{84}$	$4.44\ 10^{20}$
7	$3\ 10^{26}$	$3\ 10^{20}$	$3\ 10^{8}$	$2.00\ 10^{53}$	$2.00\ 10^{77}$	$2.00\ 10^{77}$	$1.80\ 10^{70}$	$1.80\ 10^{94}$	$1.80\ 10^{94}$	$2.96\ 10^{26}$
8	$4\ 10^{26}$	$9\ 10^{20}$	$3\ 10^{8}$	$4.05\ 10^{54}$	$3.64\ 10^{79}$	$3.64\ 10^{79}$	$3.64\ 10^{71}$	$3.28\ 10^{96}$	$3.28\ 10^{96}$	$6.00\ 10^{27}$
9	$5\ 10^{26}$	$3\ 10^{21}$	$3\ 10^{8}$	$1.20\ 10^{56}$	$1.20\ 10^{82}$	$1.20\ 10^{82}$	$1.08\ 10^{73}$	$1.08\ 10^{99}$	$1.08\ 10^{99}$	$1.77\ 10^{29}$

a) In item 1 of the Table 1, for the following parameters, T = 10^{13} K, C_G = C = $3 10^8$ m/s, calculating we get the following values:

m = $6\ 10^{30}$ kg, baryonic mass.

δ = 0, dark matter mass.

 doi:10.20944/preprints202408.0101.v1

$M = m = 6\ 10^{30}$ kg

$Rs = 8.89\ 10^{3}$ m, Schwarzschild radius.

b) In item 9 of the Table 1, for the following parameters, $T = 5\ 10^{26}$ K, $C_G = 3\ 10^{21}$ m/s, $C = 310^{8}$ m/s, calculating we get the following values:

$m = 1.20\ 10^{56}$ kg, baryonic mass.

$\delta = 1.20\ 10^{82}$ kg, dark matter mass.

$M = \delta = 1.20\ 10^{82}$ kg

$Rs = 1.77\ 10^{29}$ m, Schwarzschild radius.

c) It is important to emphasize, for the time t equal to 5τ, at the moment the disintegration of the black hole occurs, the big bang originates, the total baryonic mass of the universe corresponds to $m = 10^{56}$ kg.

d) It is important to highlight, for time t equal to 5τ, at the moment in which the disintegration of the black hole occurs, the big bang originates, the total mass of the dark matter of the universe corresponds to $\delta = 10^{82}$ kg.

It is important to highlight the following, when scientists calculated the total baryon mass of the universe, they gave them the following value $m = 10^{54}$ kg, in our calculation, the total baryon mass of the universe gave the following value, $m = 10^{56}$ kg; 100 times greater, I think the difference between the calculations is in the order taking into account the complexity of the calculation.

Figure 16, shows the growth of the tau (τ) constant, as a function of speed vs. temperature.

If we look at Figure 15, we see that the upper and lower ring singularity are formed by positively charged bosons.

If we consider the electric field E, both (ring singularity) exert a repulsive force. If we consider the magnetic field B, both (ring singularity) exert a repulsive force. Therefore, the only force holding the black hole together is the gravitational force. Above the critical mass of the black hole, the force of repulsion of the electric field and the magnetic field Fr is greater than the force of gravitational attraction Fg, the disintegration of the black hole occurs, that is, a white hole is produced. What we call the Big Bang, this process gives rise to cosmic inflation.

Next, we are going to explain the process that gives rise to cosmic inflation.

Cosmic Inflation

Let's look at Figure 17 and 20, consider that we move only in the vertical Y time axis, the X axis of space is null. If we consider the instant of time To^{-}, we observe that we are in a black hole; If we consider the instant of time To^{+}, we observe that we are in a white hole. The instant of time To is an inflection point at which the transition from a black hole to a white hole occurs.

Now let's consider a test particle (1) that moves in the X axis, the Y time axis is null. We begin our movement on the right side through the parallel antiverse, we continue to the left and cross the region of the parallel wormhole, until we reach the inflection point.

Now let's consider a test particle (2) that moves in the X axis, the Y time axis is null. We begin our movement on the left side along the antiverse, we continue to the right, we cross the wormhole region, until we reach the inflection point X.

Let us observe that the test particles (1) and the test particle (2) are at the inflection point, but cannot exceed it.

Now, if we analyse the inflection point, we see that it is a space-type point, its trajectory is space-type, this implies that in order to cross it we need to move at a speed greater than the speed of light, $v > c$.

If we analyse section 2.9, Antiverse; We see that there is a region for negative radii, $r < 0$ which corresponds to a negative mass, $M < 0$.

Later we will analyse the importance of negative mass.

Now we will analyse Figure 15, we will use two test particles for our analysis, the test particle (1) and the test particle (2). We will consider that the test particle (1) is directed towards the upper singularity ring and the test particle (2) is directed towards the lower singularity ring.

 doi:10.20944/preprints202408.0101.v1

The test particle (1) that is in the upper singularity ring cannot go to the lower singularity ring.

The test particle (2) that is in the lower singularity ring cannot go to the upper singularity ring.

Therefore, in the black hole model represented in Figure 15, there is also an inflection point.

Here, we are going to hypothesize that the black hole reaches its critical mass Mc, collapses, disintegrates and transforms into a white hole, this process generates cosmic inflation.

This is the only condition in which a test particle can cross the inflection point whose velocity v > c.

If we look at Figure 20, at time To, the amount of matter in the black hole is the same as that of the white hole. We can deduce this by comparing the orange triangle with the yellow triangle.

There is a second condition in which a test particle can cross the inflection point, it is when a black hole behaves like a quasar, generating relativistic jets. In this condition that we have already analyzed, the inflection point exhibits a feedback inflationary instability, which is what generates the relativistic jets and occurs for the condition $M^2 < Q^2 + a^2$

Now we are going to analyse the importance of negative mass, M < 0 (Antiverse), in the origin of cosmic inflation.

We said that the mass of a black hole can be represented in analogy to that of an RC circuit as follows:

$$M = m - i\delta \qquad (57)$$

Where M is the total mass of a black hole, m is the baryonic mass; δ corresponds to dark matter and (i) is the irrational number √(-1).

We can represent this equation in the following way:

$$M = m + i(-\delta) \qquad (58)$$

In equation 58, we see that the mass of dark matter can be represented as a negative mass.

We said that a black hole grows like a capacitor, following the Tau constant.

$$\tau = RC \qquad (59)$$

In item 9 of the Table 1, for the following parameters, T = 5 10^{26} K, C_G = 3 10^{21} m/s, C = 3$10^8$ m/s, calculating we get the following values:

m = 1.20 10^{56} kg, baryonic mass.

δ = 1.20 10^{82} kg, dark matter mass.

M = δ = 1.20 10^{82} kg

Rs = 1.77 10^{29} m, Schwarzschild radius.

These values correspond to the moment of time To, in which the black hole reaches its critical mass Mc, collapses, disintegrates, transforming into a white hole.

We will use these values to calculate your Plank Length.

Table 3. - Calculations of Planck parameters as a function of C_G.

Range	Minimum value	Maximum value	Units
Velocity C_G	3 10^8	3 10^{21}	m/s
Planck`s length Lp	1.28 10^{-54}	1.61 10^{-35}	m
Planck`s time tp	0.42 10^{-75}	5.39 10^{-44}	s
Planck`s temperature T	1.41 10^{32}	0.62 10^{90}	K

At instant To, the Planck length inside a black hole (white hole) corresponds to Lp = 1.28 10^{-54} m.

If we consider the Planck length Lpε, the minimum length of space-time, like a spring and due to the action of v > c (300,000 km/s), this length decreases in values of Lpɢ, that is, Lpɢ < Lpε, allowing us to imagine the immense forces involved in compressing space-time of length Lpε into smaller values of space-time Lpɢ. The immense energy stored and released in the spring of length Lpɢ, to recover its initial length Lpε, is the cause of the exponential expansion of space-time in the first moments of the Big Bang.

At time T0, when the black hole disintegrates and the Big Bang occurs, roughly all matter was dark matter, relativistic dark matter. This is represented in equation (52).

4.2. Inside a Black Hole

 doi:10.20944/preprints202408.0101.v1

We are going to use the paper: Proton decay and inverse neutron decay, we will use the new particles proposed in this article to determine what really exists inside black holes.

The new proposed particles are the following:

- Dproton
- Protoniu
- Dneutron
- Neutroniumd

In the following Figure we are going to present the main characteristics of these particles along with those of the proton and the neutron for comparison.

	NEUTRON		PROTÓN		DPROTON		PROTONIU
MASS (MeV/c²)	939.56		938.27		651.78		253.44
MASS (Kg)	$1.675\ 10^{-27}$		$1.672\ 10^{-27}$		$1.16\ 10^{-27}$		$4.51\ 10^{-28}$
ENERGY (J)	$15.06\ 10^{-11}$		$15.03\ 10^{-11}$		$10.4\ 10^{-11}$		$4.06\ 10^{-11}$
FRECUENCY (Hz)	$2.27\ 10^{23}$		$2.26\ 10^{23}$		$1.57\ 10^{23}$		$0.61\ 10^{23}$
TEMPERATURE (K)	$10.91\ 10^{12}$		$10.89\ 10^{12}$		$7.53\ 10^{12}$		$2.89\ 10^{12}$
	DNEUTRON		NEUTRON		NEUTRONIUMD		
MASS (MeV/c²)	1140.33		939.56		443.10		
MASS (Kg)	$2.03\ 10^{-27}$		$1.675\ 10^{-27}$		$7.89\ 10^{-28}$		
ENERGY (J)	$18.27\ 10^{-11}$		$15.06\ 10^{-11}$		$7.09\ 10^{-11}$		
FRECUENCY (Hz)	$2.75\ 10^{23}$		$2.27\ 10^{23}$		$1.06\ 10^{23}$		
TEMPERATURE (K)	$13.23\ 10^{12}$		$10.91\ 10^{12}$		$5.13\ 10^{12}$		

Figure 21 Characteristic parameters of the following particles: Neutron, Proton, Dproton, Protoniu, Dneutron and Neutroniumd.

We said that the collapse of a star of more than 25 solar masses produces a black hole of 3 solar masses.

In section 3, *Modelling of a black hole*; we calculated the equivalent neutron/black hole model, which gave us an equivalent neutron mass of 300 MeV/c².

BLACK HOLE												
		INTERACTION 1				INTERACTION 2						
RBG		R	B	G		R	R	B	B	G	G	
DDU		D	D	U		D	D	D	D	U	U	
DDU		D	D	U		D	U	D	U	D	D	
RBG		R	B	G		B	G	R	G	R	B	
m(Mev/c^2)	300.60	0				300.60						
		0	0	0		28.54	60.88	28.54	60.88	60.88	60.88	

Figure 22. - Equivalent Neutron/ Black Hole.

Taking into account the above and considering the equivalent neutron/black hole model, we are going to hypothesize that the collapse of a star larger than 25 suns produces a black hole of 3 solar masses, which contains the neutroniumd particle inside.

We are going to show the graph of the *neutroniumd* particle:

NEUTRONIUMD												
		INTERACTION 1				INTERACTION 2						
RBG		R	B	G		R	R	B	B	G	G	
DDU		D	D	D		D	D	D	D	D	D	
DDU		D	D	D		D	D	D	D	D	D	
RBG		R	B	G		B	G	R	G	R	B	
m(Mev/c²)	443.10	0				443.10						
		0	0	0		73.85	73.85	73.85	73.85	73.85	73.85	

Figure 23 Neutroniumd.

 doi:10.20944/preprints202408.0101.v1

If we look at Figure 23, the *neutroniumd* particle is made up of three D quarks, matter, it does not contain antimatter; the configuration of these three D quarks is analogous to that of an electric generator, that is to say that each quark can be represented by three vectors out of phase by 120 degrees whose vector sum is zero and whose scalar sum is (-1).

As seen in Figure 23, the *neutroniumd* particle has a mass of 443.10 MeV/c².

The scalar charge of the *neutroniumd* particle is (-1) but the vectorial charge is zero (0). In other words, the black hole would be formed by negatively charged particles but whose vector sum is zero (0). The distribution of the D-quark vectors inside the black hole is such that the resulting charge on the black hole is zero (0).

In the following graph, we are going to represent the black hole model formed by *neutromiumd* particles.

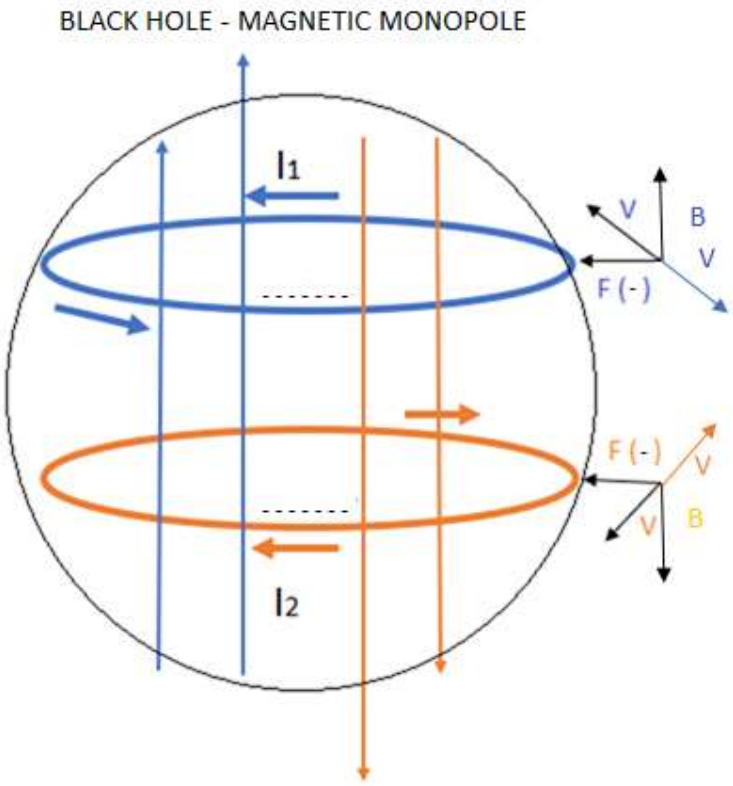

Figure 24. - black hole formed by *Neutroniumd* particles.

It can be seen in Figure 24 that negatively charged particles enter the black hole and positively charged particles are repelled from the black hole.

At this stage, the black hole grows by devouring negatively charged particles.

As the black hole grows, the mass, pressure, density, etc. increases and another transformation occurs inside the black holes.

We are going to analyse the following transformation that happens inside black holes.

Let's hypothesize the following, as a black hole grows and reaches a critical point of pressure, volume, temperature, density, etc., the neutroniumd particle decays into the protoniu particle.

This decay of the *neutroniumd* particle in the *protoniu* particle is very important and explains the jets that quasars produce.

 doi:10.20944/preprints202408.0101.v1

PROTONIU												
		INTERACTION 1				INTERACTION 2						
RBG		R	B	G		R	R	B	B	G	G	
UUU		U	U	U		U	U	U	U	U	U	
UUU		U	U	U		U	U	U	U	U	U	
RBG		R	B	G		B	G	R	G	R	B	
m(Mev/c²)	253.44	0				253.44						
		0	0	0		42.24	42.24	42.24	42.24	42.24	42.24	

Figure 25 *Protoniu.*

If we compare Figure 23 and 25, we observe that the mass of the Neutroniumd particle is 443 MeV/c² and the mass of the protoniu particle is 253 MeV/c².

We observe that the D quarks have to decay into U quarks, this is analogous to β^- decay, therefore electrons, antineutrinos and electromagnetic energy will be produced.

Neutroniumd → protoniu + e^- + $\tilde{\nu}$ + ΔE

Quark D → Quark U + e^- + $\tilde{\nu}$ + ΔE

Inside a black hole the *neutroniumd* particle decays into the *protoniu* particle.

Electrons, antineutrinos and electromagnetic radiation are sent in the jet, this would explain why the jet particles are so collimated.

The relativistic jet could be explained for the condition $M^2 < Q^2 + a^2$, in which there is a naked singularity.

Along with the jet, we must include the particles that are expelled by the action of the magnetic field of the accretion disk.

When the black hole is formed by the *neutroniumd* particle, the magnetic field B, forces negative particles into the interior of the black hole.

When the black hole is formed by the *protoniu* particle, the magnetic field B, forces positive particles to enter the interior of the black hole.

In other words, we have black holes formed by negative charges *neutroniumd* and black holes formed by positive charges *protoniu.*

According to this theory, the relativistic jet of quasars is produced when the *neutroniumd* particles, formed by the D quark, decay into the *protoniu* particle, formed by the U quark, inside the black hole.

If we compare Figure 22 - Equivalent Neutron/ Black Hole with Figure 25 - protoniu; We observe that the masses are approximately equal (300 ≈ 253) Mev/c².

In the following graph, we are going to represent the black hole model formed by *protoniu* particles.

 doi:10.20944/preprints202408.0101.v1

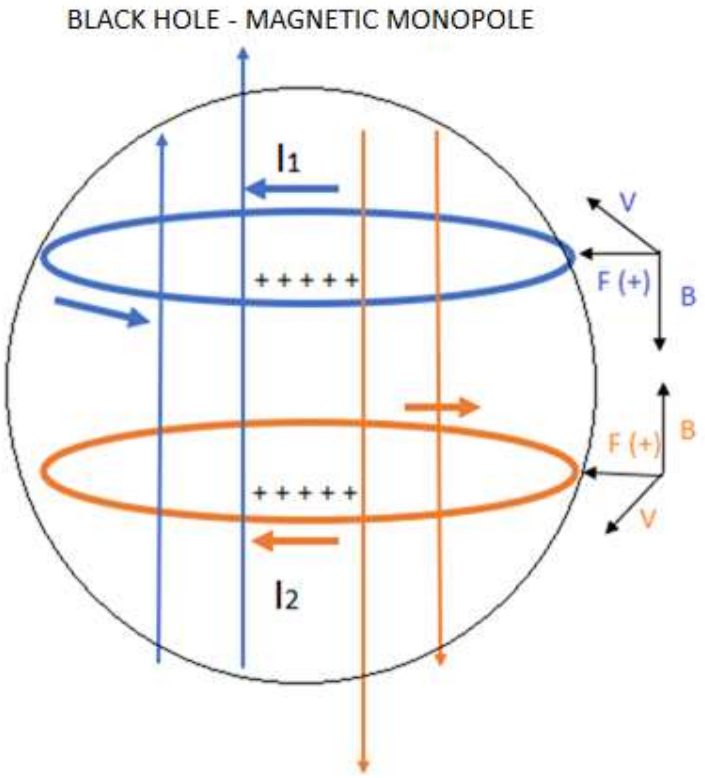

Figure 26. - black hole model formed by *protoniu* particles.

Black holes can be formed by negatively charged particles (*neutroniumd*) or positively charged particles (*protoniu*), however, it is important to know that the net charge of black holes is zero, due to their vector configuration, whether they are formed by positively or negatively charged particles.

Another important characteristic of black holes is that they are formed by matter and do not contain antimatter, the process of formation of a black hole separates matter from antimatter.

If we look at Figure 13, 15, 24 and 26; We see that we write 'Black Hole / Magnetic Monopole', this is due to the following: if we carefully analyse our black hole model, they behave the same as magnetic monopoles.

4.3. Generalization: Neutron Stars

We are going to use the paper: *Proton decay and inverse neutron decay*, we will use the new particles proposed in this article to determine what really exists inside neutron star.

The new proposed particles are the following:

- Dproton
- Protoniu
- Dneutron
- Neutroniumd

In current physics we talk about neutron stars composed of neutrons and quark plasma in their core.

In the following figures we are going to propose the particles with which we are going to work:

 doi:10.20944/preprints202408.0101.v1

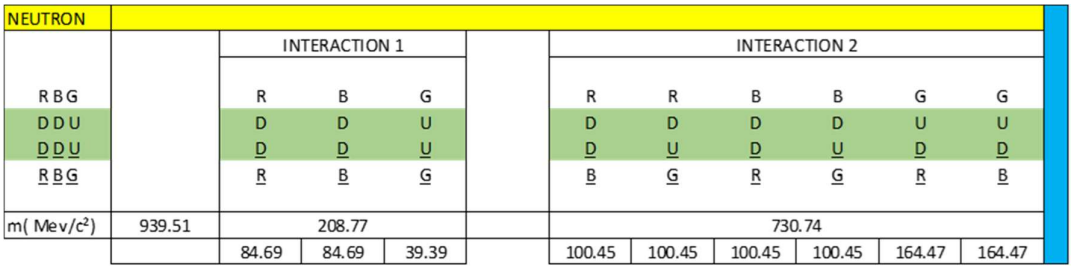

NEUTRON												
		INTERACTION 1				INTERACTION 2						
R B G		R	B	G		R	R	B	B	G	G	
D D U		D	D	U		D	D	D	D	U	U	
D D U		D	D	U		D	U	D	U	D	D	
R B G		R	B	G		B	G	R	G	R	B	
m(Mev/c²)	939.51	208.77				730.74						
		84.69	84.69	39.39		100.45	100.45	100.45	100.45	164.47	164.47	

Figure 27 Neutron.

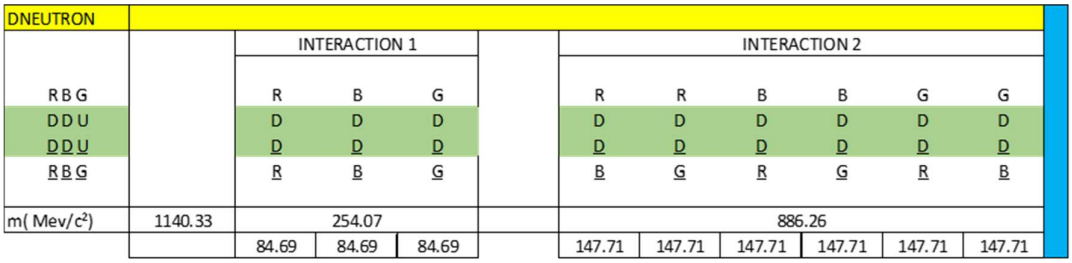

DNEUTRON												
		INTERACTION 1				INTERACTION 2						
R B G		R	B	G		R	R	B	B	G	G	
D D U		D	D	D		D	D	D	D	D	D	
D D U		D	D	D		D	D	D	D	D	D	
R B G		R	B	G		B	G	R	G	R	B	
m(Mev/c²)	1140.33	254.07				886.26						
		84.69	84.69	84.69		147.71	147.71	147.71	147.71	147.71	147.71	

Figure 28 Dneutron.

Taking into account the particles of Figure 27 (neutron) and Figure 28 (Dneutron), we are going to propose the following:

We are going to hypothesize that inside neutron stars, neutrons can decay into Dneutron particles, this would be the cause of the jets that produce magnetars or pulsars.

Let us remember that unlike black holes that behave like magnetic monopoles, neutron stars behave like magnetic dipoles.

The particles that form black holes are composed solely of matter; they do not contain antimatter.

The particles that make up neutron stars are composed of matter and antimatter.

Table 1. - Calculation of the interactions in MeV/c², when the neutron decay in the Dneutron particle.

INVERSE NEUTRON DECAY			
NEUTRON	DNEUTRON	INTERACTION	INTERACTION (MeV/c²)
R(DD)R	R(DD)R	E1 = 0	E1 = 0
B(DD)B	B(DD)B	E2 = 4.6	E2 = 45.29
G(UU)G	G(DD)G	E3 = 4.6	E3 = 45.29 (-)
R(DD)B	R(DD)B	E4 = 10	E4 = 98.47
R(DU)G	R(DD)G	E5 = 10	E5 = 98.47 (+)
B(DD)R	B(DD)R	E6 = 4.7	E6 = 46.28
B(DU)G	B(DD)G	E7 = 4.7	E7 = 46.28 (+)
G(UD)R	G(DD)R	E8 = 5.0	E8 = 49.23 (-)
G(UD)B	G(DD)B	E9 = 5.0	E9 = 49.23 (-)
TOTAL INTERACTION			IEtI = 478.54 MeV/c²
$(W^+)e^+$ INTERACTION			IEeI = W^+ = 1.00 MeV/c²
$(Z^0)n$ INTERACTION			IEnI = 52.19 MeV/c²
$(Z^0)p$ INTERACTION			IEpI = 45.29 MeV/c²
(Z^0) INTERACTION			IZ^0I = 6.90 MeV/c²
Θ angle, Θ = arc cos W^+/Z^0			Θ = 82^0

 doi:10.20944/preprints202408.0101.v1

It is important to highlight that the decay of the neutron in the Dneutron particle produces a total interaction of Et = 478.54 MeV/c², this would be the cause of the jets that produce magnetars or pulsar.

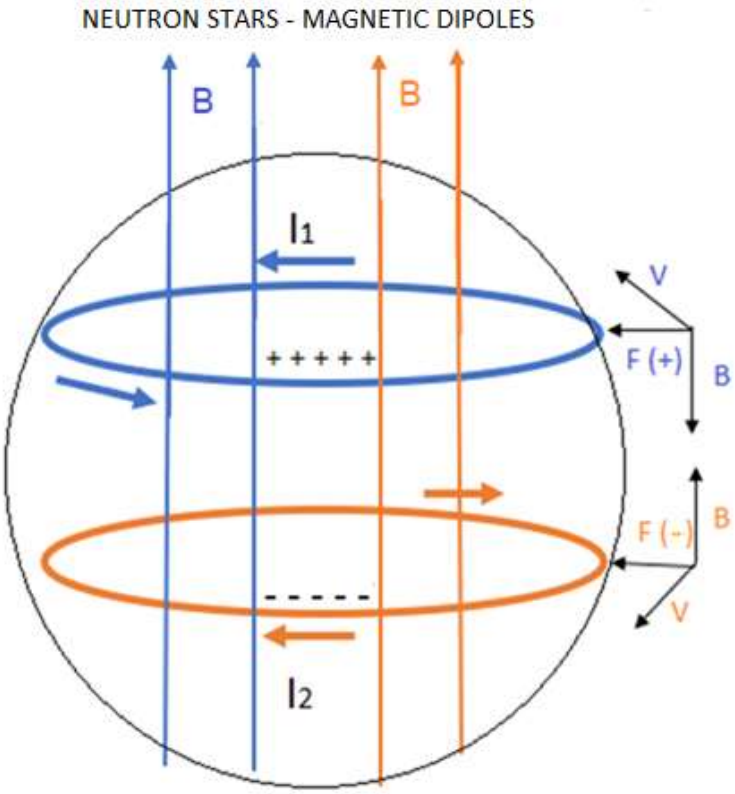

Figure 29 Neutron stars.

5. Conclusions

We have shown that the interpretation of the Kerr-Newman diagram and the theory: RLC electrical modelling of a black hole and the early universe, are equivalent; To do this, we have generated a black hole model which we represent in Figure 13. Our black hole model is characterized by the fact that it can rotate and is also positively charged.

To demonstrate this equivalence between both theories, we have focused on the interpretation for the following conditions; $M^2 > Q^2 + a^2$, $M^2 = Q^2 + a^2$ and $M^2 < Q^2 + a^2$, with a special focus placed on the condition in which the black hole reaches its critical mass M = Mc.

For M = Mc, we have demonstrated the growth curve of a black hole, following the curve of the Tau constant, in analogy to that of an RC circuit. A black hole is born, grows and collapses until it disintegrates and produces a white hole. All calculations are represented in Table 2 and Figure 16.

We have generalized our proposed black hole model. In Figure 23 and 24, we have proposed a rotating and negatively charged black hole which is formed by *neutroniumd* particles. In Figure 25 and 26, we have proposed a rotating and positively charged black hole which is formed by *protoniu* particles.

It is necessary to make it clear that when a black hole originates, it is generally formed by a negative charge. As it grows, it reaches a critical point in which the *neutroniumd* particles (formed by D quark) decay into the protoniu particle (formed by quark U); This process generates relativistic jets and we generally call these black holes quasars.

Finally, we have extended our proposal and presented a model for neutron stars.

Conflicts of Interest: The author declares that there are no conflicts of interest.

References

1. Flores, H. G. (2023). RLC electrical modelling of black hole and early universe. Generalization of Boltzmann's constant in curved spacetime. J Mod Appl Phys. 2023; 6(4):1-6. https://www.pulsus.com/scholarly-articles/rlc-electrical-modelling-of-black-hole-and-early-universe-generalization-of-boltzmanns-constant-in-curved-spacetime.pdf https://sites.ifi.unicamp.br/sobreira/files/2018/07/mestrado-tanderson.pdf
2. Peter Cameron The Penrose Property with a Cosmological Constant Department of Applied Mathematics and Theoretical Physics, University of Cambridge. https://arxiv.org/abs/2106.02536
3. Roy. P. Kerr, Do Black Holes have Singularities? University of Canterbury, Christchurch; Lifschitz Prof. ICRANet, Pescara. December 5, 2023 https://arxiv.org/pdf/2312.00841.pdf
4. J C Schindler, A Aguirre Algorithms for the explicit computation of Penrose diagrams Department of Physics, University of California Santa Cruz, Santa Cruz, CA, USA https://arxiv.org/pdf/1802.02263
5. Andrew Strominger Les Houches Lectures on Black Holes Department of Physics, University of California, Santa Barbara, CA 93106-9530 https://arxiv.org/pdf/hep-th/9501071
6. Black Holes University of Cambridge https://www.damtp.cam.ac.uk/user/tong/gr/six.pdf
7. Chapter 21. Inside the Spinning Black Hole Edwin F. Taylor https://www.eftaylor.com/exploringblackholes/Ch21TravelThroughTheSpinningBH170831v1.pdf
8. Andrew J. S. Hamilton General Relativity, Black Holes, and Cosmology University of Colorado Boulder https://jila.colorado.edu/~ajsh/astr3740_17/grbook.pdf
9. Steven B. Giddings The Black Hole Information Paradox Department of Physics, University of California, Santa Barbara, CA 93106-9530 https://www.nevis.columbia.edu/~zajc/acad/W3072/9508151.pdf
10. V.M. Khatsymovsky On the discrete version of the Kerr–Newman solution Budker Institute of Nuclear Physics of Siberian Branch Russian Academy of Sciences, Novosibirsk, 630090, Russia https://arxiv.org/pdf/2212.13547v2
11. Tim Adamo (a) and E. T. Newman (b) The Kerr-Newman metric: A Review Department of Applied Mathematics & Theoretical Physics, University of Cambridge. Department of Physics & Astronomy, University of Pittsburgh. https://arxiv.org/pdf/1410.6626
12. Alexander Shatskiy Analysis of the Topology of the Kerr Metric https://arxiv.org/pdf/2004.14156
13. Ashok B. Joshi,1, ∗ Divya Tahelyani,1, † Dipanjan Dey,2, ‡ and Pankaj S. Joshi3, 1, Observational aspects of a class of Dark matter spacetimes 1 International Centre for Cosmology, Charusat University, Anand, GUJ 388421, India 2Department of Mathematics and Statistics, Dalhousie University, Halifax, Nova Scotia, Canada, B3H 3J5 3Cosmology Centre, Ahmedabad University, Ahmedabad, GUJ 380009, India https://arxiv.org/pdf/2212.03042
14. Rohan Kulkarni Black Holes, Singularity Theorems & The Global Structure of Spacetimein General Relativity Elementary Particle Theory, Institute of Theoretical Physics, University of Leipzig https://arxiv.org/pdf/1911.06608
15. Eugene Terry Tatum Black Hole Complementarity in Terms of the Outsider and Insider Perspectives Independent Researcher, Bowling Green, Kentucky, USA https://www.scirp.org/pdf/jmp_2024020815045386.pdf
16. Andrew Walcott Beckwith Penrose Suggestion as to Pre Planck-Era-Black Holes Showing Up in Present Universe Data Sets Discussed, with a Possible Candidate as to GW Radiation Which May Provide Initial CMBR Data. Physics Department, Chongqing University, Chongqing, China https://www.scirp.org/pdf/jhepgc_2021082709305290.pdf
17. W. Y. Ai, Non-singular black hole in two-dimensional asymptotically flat spacetime, Phys. Rev. D 104 (2021), no. 4, 044064.
18. B. Carter, The complete analytic extension of the Reissner-Nordström metric in the special case e2 = m2, Physics Letters 21 (1966), no. 4, 423–424.
19. V. P. Frolov and A. Zelnikov, Introduction to black hole physics, Oxford Univ. Press, Oxford, 2011.
20. S. W. Hawking and G. F. R. Ellis, The large-scale structure of space-time, Cambridge Monographs on Mathematical Physics, No. 1, Cambridge University Press, London-New York, 1973.
21. J. M. Maldacena, The Large N limit of super conformal field theories and supergravity, Adv. Theor. Math. Phys. 2 (1998), 231–252.
22. A. S. Wright, The Advantages of Bringing Infinity to a Finite Place: Penrose Diagrams as Objects of Intuition, Historical Studies in the Natural Sciences 44 (2014), no. 2, 99–139.
23. JEFF STEIHAUER. Observation of quantum Hawking radiation and its entanglement in an analogue black hole. https://arxiv.org/abs/1510.00621
24. JEFF STEIHAUER. Spontaneous Hawking radiation and beyond: Observing the time evolution of an analogue black hole https://arxiv.org/abs/1910.09363
25. J.S.Farnes A Unifying Theory of Dark Energy and Dark Matter: Negative Masses and Matter Creation within a Modified ΛCDM Framework. https://arxiv.org/abs/1712.07962

26. Alberto Casas, Profesor de Investigación IFT, CSIC/UAM. La luz y el origen de la materia. https://www.youtube.com/watch?v=CTrX_JBNEnU
27. Iván García Brao. Ecuación de campo de Einstein, Universidad de Murcia, Facultad de Matemáticas. Trabajo de grado año 2018. https://www.um.es/documents/118351/9850492/Garc%C3%ADa+Brao+TF_77837970.pdf/debaa03b-605b-420d-b3ac-85549b6622c0
28. Luis Felipe de Oliveira Guimarães, Orientadora Maria Emilia Xavier Guimarães. Soluciones de buracos negros na relatividade general, Universidad federal Fluminense, Bacherelado em Física. Trabajo de grado 2015. https://app.uff.br/riuff/bitstream/handle/1/5977/Luiz%20Filipe%20Guimaraes.pdf;jsessionid=4EAAF6CB7A4B776D04C9E6E6573D5919?sequence=1
29. Kostas kokkotas, Field Theory.
30. James B. Hartle, Gravity and introduction to Einstein´s General Relativity.
31. Charles W. Misner, Kip S. Thorne and Jhon Archibald Wheelher, Gravitation.
32. Benito Marcote, Cosmologia Cuantica y creacion del universe.
33. Carlos Rovelli, Quantum Gravity.
34. Vinicius Miranda Bragança, Singularidades em teorias f(r) da gravitação. http://arcos.if.ufrj.br/teses/mestrado_vinicius_miranda.pdf
35. Laurent Pitre ∗, Mark D. Plimmer, Fernando Sparasci, Marc E. Himbert; 2019. Determinations of the Boltzmann constant. https://hal.science/hal-02166573/file/1-s2.0-S1631070518301348-main.pdf
36. ZEUS Collaboration, 2016. Limits on the effective quark radius from inclusive ep scattering at HERA. Accepted for publication in Physics Letters B. https://arxiv.org/pdf/1604.01280.pdf
37. Flores, H. G.; Gonçalvez de Souza, M. I. Theory of the Generalization of the Boltzmann's Constant in Curved Space-Time. Shannon-Boltzmann Gibbs Entropy Relation and the Effective Boltzmann's Constant. Preprints 2023, 2023090301. https://doi.org/10.20944/preprints202309.0301.v1
38. Bernard Carr, and Florian Kühnel - Annual Review of Nuclear and Particle Science. Primordial Black Holes as Dark Matter: Recent Developments https://www.annualreviews.org/doi/10.1146/annurev-nucl-050520-125911
39. D. T. Son - University of Washington. AdS/CFT correspondence and the Quark-Gluon Plasma https://www.phenix.bnl.gov/WWW/publish/jfrantz/ou_nucl_lunch/DamTSon_lectures.pdf
40. Marc Kamionkowski and Adam G. Riess. The Hubble tension and Early Dark Energy https://arxiv.org/pdf/2211.04492.pdf
41. Luis Anchordoqui, Carlos Nuñez and Kasper Olsen Quantum cosmology and AdS/CFT https://arxiv.org/abs/hep-th/0007064
42. Jefferson Londoño and Eduardo Velasquez. Agujeros Negros de Kerr Escuela de Fsica, Universidad Nacional de Colombia https://www.researchgate.net/publication/328380970_Agujeros_Negros_de_Kerr
43. Flores, H. G.; Gonçalves de Souza, M. I. RC Electrical Modelling of Black Hole. New Method to Calculate the Amount of Dark Matter and the Rotation Speed Curves in Galaxies. Preprints 2023, 2023092017. https://doi.org/10.20944/preprints202309.2017.v1
44. Roger Penrose THE ROAD TO REALITY. A Complete Guide to the Laws of the Universe First published in Great Britain in 2004 by Jonathan Cape https://chaosbook.org/library/Penr04.pdf
45. Edmund Bertschinger & Edwin F. Taylor Inside the Spinning Black Hole, CHAPTER 21 https://www.eftaylor.com/exploringblackholes/Ch21TravelThroughTheSpinningBH170831v1.pdf
46. H. Nagakura and S. Yamada, The standing accretion shock instability in the disk around the Kerr black hole, The Astrophysical Journal 696, 2026 (2009).
47. P. Tarafdar, S. Maity, and T. K. Das, Influence of flow thickness on general relativistic low angular momentum accretion around spinning black holes, Phys. Rev. D 103, 023023 (2021).
48. V. Moncrief, Stability of stationary, spherical accretion onto a Schwarzschild black hole, Astrophysical Journal 235, 1038 (1980).
49. P. Tarafdar and T. K. Das, Influence of the geometric configuration of accretion flow on the black hole spin dependence of relativistic acoustic geometry, International Journal of Modern Physics D 27, 1850023 (2018).
50. M. A. Shaikh and T. K. Das, Linear perturbations of low angular momentum accretion flow in the Kerr metric and the corresponding emergent gravity phenomena, Phys. Rev. D 98, 123022 (2018).
51. B. Carter, Complete analytic extension of the symmetry axis of Kerr's solution of Einstein's equations, Phys. Rev. 141, 1242 (1966).
52. B. Carter, Global structure of the Kerr family of gravitational fields, Phys. Rev. 174, 1559 (1968).
53. P. Tarafdar, D. A. Bollimpalli, S. Nag, and T. K. Das, Influence of geometrical configuration on low angular momentum relativistic accretion around rotating black holes, Phys. Rev. D 100, 043024 (2019).
54. M. A. Abramowicz, A. Lanza, and M. J. Percival, Accretion disks around Kerr black holes: Vertical equilibrium revisited, The Astrophysical Journal 479, 179 (1997).
55. S. W. Hawking, "Breakdown of predictability in gravitational collapse," Phys. Rev. D 14, 2460 (1976).

56. L. Susskind, L. Thorlacius and J. Uglum, "The Stretched horizon and black hole complementarity," Phys. Rev. D 48, 3743 (1993) [hep-th/9306069].
57. D. Marolf and J. Polchinski, "Gauge/Gravity Duality and the Black Hole Interior," Phys. Rev. Lett. 111, 171301 (2013) [arXiv:1307.4706 [hep-th]].
58. J. Maldacena and L. Susskind, "Cool horizons for entangled black holes," Fortsch. Phys. 61, 781 (2013) [arXiv:1306.0533 [hep-th]].
59. M. R. Mbonye and D. Kazanas, "Non-singular black hole model as a possible end product of gravitational collapse," Phys. Rev. D 72, 024016 (2005); "Can Gravitational Collapse Sustain Singularity-Free Trapped Surfaces?" Int. J. Mod. Phys. D 17, 165 (2008)
60. V. P. Frolov, "Notes on non-singular models of black holes," Phys. Rev. D 94, no. 10, 104056 (2016) [arXiv:1609.01758 [gr-qc]].
61. V. P. Frolov and A. Zelnikov, "Quantum radiation from an evaporating non-singular black hole," Phys. Rev. D 95, no. 12, 124028 (2017) [arXiv:1704.03043 [hep-th]].
62. J. B. Hartle, "Tidal Friction in Slowly Rotating Black Holes," Phys. Rev. D 8, 1010 (1973).
63. R. Brustein, A. J. M. Medved and K. Yagi, "When black holes collide: Probing the interior composition by the spectrum of ringdown modes and emitted gravitational waves," Phys. Rev. D 96, no. 6, 064033 (2017) [arXiv:1704.05789 [gr-qc]].
64. R. Carballo-Rubio, F. Di Filippo, S. Liberati and M. Visser, "Phenomenological aspects of black holes beyond general relativity," Phys. Rev. D 98, no. 12, 124009 (2018) doi:10.1103/PhysRevD.98.124009 [arXiv:1809.08238 [gr-qc]].
65. Richard A. Matzner, Texas Cosmology Centre, University of Texas at Austin The Kerr-de Sitter Universe https://arxiv.org/pdf/1011.0479
66. Middleton, M.: Black hole spin: theory and observation, Chapter 3. In: Bambi, C. (ed.) Astrophysics of Black Holes: From Fundamental Aspects to Latest Developments, pp. 99–151. Springer, Berlin (2016)
67. Gou, L., McClintock, J.E., Reid, M.J., Orosz, J.A., Steiner, J.F., Narayan, R., Xiang, J., Remillard, R.A., Arnaud, K.A., Davis, S.W.: The extreme spin of the black hole in Cygnus X-1. Astrophys. J. 742, 85 (2011). https://doi.org/10.1088/0004-637X/742/2/85
68. Stuchlík, Z., Slaný, P.: Equatorial circular orbits in the Kerr–de Sitter spacetimes. Phys. Rev. D 69, 064001 (2004). https://doi.org/10.1103/PhysRevD.69.064001
69. de Felice, F., Calvani, M.: Causality violation in the Kerr metric. Gen. Relativ. Gravit. 10, 335–342 (1979). https://doi.org/10.1007/BF00759491
70. Hackmann, E., Lämmerzahl, C., Kagramanova, V., Kunz, J.: Analytical solution of the geodesic equation in Kerr–(anti) de Sitter space-times. Phys. Rev. D 81, 044020 (2010). https://doi.org/10.1103/PhysRevD.81.044020
71. Stuchlík, Z., Hledík, S.: Some properties of the Schwarzschild-de Sitter and Schwarzschild-anti-de Sitter spacetimes. Phys. Rev. D 60, 044006 (1999). https://doi.org/10.1103/PhysRevD.60.044006
72. Gerardo Flores, H.; Jain, H.; Gonçalves de Souza, M. I. Proton Decay and Inverse Neutron Decay. Preprints 2024, 2024050023. https://doi.org/10.20944/preprints202405.0023.v1
73. Flores, H. G.; Jain, H.; Gonçalves de Souza, M. I. Origin of the Dark Energy. Preprints 2024, 2024051639. https://doi.org/10.20944/preprints202405.1639.v1
74. Gerardo Flores, H.; Gonçalves de Souza, M. I. Electrical-Quantum Modelling of the Neutron and Proton as a Three-Phase Alternating Current Electrical Generator. Determination of the Number of Quarks-Antiquarks-Gluons and Gravitons, Inside a Neutron. Preprints 2023, 2023102076. https://doi.org/10.20944/preprints202310.2076.v2